



Stockholms  
universitet

Denna digitala kopia är tillgängliggjord av Stockholms  
universitetsbibliotek enligt avtal med avtalslicensverkan som  
ingått med upphovsrättsorganisation.  
Får användas i enlighet med gällande lagstiftning.

This digital copy is provided by Stockholm University Library by  
extended collective licence in agreement with a Reproduction  
Rights Organization.  
May be used according to current laws.

# Light propagation in the universe

Edvard Mörtsell



Stockholm University  
Department of Physics  
2002



# Light propagation in the universe

Edvard Mörtsell

Akademisk avhandling som för avläggande av filosofie doktorsexamen vid  
Stockholms Universitet offentligen försvaras i The Svedbergssalen  
Roslagstullsbacken 21 lördagen den 8 juni 2002 klockan 10.15.

## Abstract

Recent measurements of the distance-redshift relation of Type Ia supernovae indicates that the expansion of the universe is accelerating, possibly due to a substantial energy fraction of the universe having a negative equation of state. This is in agreement with cosmological microwave background radiation measurements showing that the geometry of the universe is close to flat and studies of large scale structure indicating that only a minor part of the total energy density is in ordinary pressure-less matter.

As the wealth of observational data increases, the viability of the hypothesis of an accelerated expansion of the universe will be tested to higher and higher accuracy. This necessitates an increased awareness of systematic effects capable of biasing the results.

In this thesis we investigate the possible effects on Type Ia supernova observations from gravitational lensing, dust extinction and the more exotic effect of photon-axion oscillations. We find that great care is needed to control and correct for these systematic effects in order to meet the required goals of future supernova surveys.

It is also shown how supernova data can be used to obtain information on the distribution of dark matter and the properties and abundances of intergalactic dust.

Fysikum  
Stockholms Universitet

Stockholm 2002  
ISBN 91-7265-455-4



# Light propagation in the universe

Edvard Mörtsell



Stockholm University  
Department of Physics  
2002

Thesis for the degree of doctor in philosophy in theoretical physics  
Department of Physics  
Stockholm University  
Sweden

© Edvard Mörtzell 2002  
ISBN 91-7265-455-4 pp i-viii,1-98 Akademitryck AB, Edsbruk

---

## Abstract

Recent measurements of the distance-redshift relation of Type Ia supernovae indicates that the expansion of the universe is accelerating, possibly due to a substantial energy fraction of the universe having a negative equation of state. This is in agreement with cosmological microwave background radiation measurements showing that the geometry of the universe is close to flat and studies of large scale structure indicating that only a minor part of the total energy density is in ordinary pressure-less matter.

As the wealth of observational data increases, the viability of the hypothesis of an accelerated expansion of the universe will be tested to higher and higher accuracy. This necessitates an increased awareness of systematic effects capable of biasing the results.

In this thesis we investigate the possible effects on Type Ia supernova observations from gravitational lensing, dust extinction and the more exotic effect of photon-axion oscillations. We find that great care is needed to control and correct for these systematic effects in order to meet the required goals of future supernova surveys.

It is also shown how supernova data can be used to obtain information on the distribution of dark matter and the properties and abundances of intergalactic dust.

## Accompanying papers

- I.** Bergström, L., Goliath, M., Goobar, A., & Mörtsell, E.,  
*Lensing effects in an inhomogeneous universe*,  
A&A., **358**, 13 (2000).
- II.** Goliath, M., & Mörtsell, E.,  
*Gravitational lensing of Type Ia supernovae*,  
Physics Letters B., **486**, 249 (2000).
- III.** Mörtsell, E., Goobar, A., & Bergström, L.,  
*Determining the fraction of compact objects in the universe  
using supernova observations*, ApJ., **559**, 53 (2001).
- IV.** Mörtsell, E., Gunnarson, C., & Goobar, A.,  
*Gravitational lensing of the farthest known supernova SN1997ff*,  
ApJ., **561**, 106 (2001).
- V.** Mörtsell, E.,  
*The Dyer-Roeder distance-redshift relation in inhomogeneous  
universes*, A&A, **382**, 787 (2002).
- VI.** Goobar, A., Bergström, L., & Mörtsell, E.,  
*Measuring the properties of extragalactic dust and implications  
for the Hubble diagram*, A&A. **384**, 1, (2002).
- VII.** Mörtsell, E., Bergström, L. & Goobar, A.,  
*Photon-axion oscillations and Type Ia supernovae*,  
arXiv:astro-ph/0202153 (2002).
- VIII.** Goobar, A., Mörtsell, E., Amanullah, R., Goliath, M.,  
Bergström, L., & Dahlén, T.,  
*SNOC: a Monte-Carlo simulation package for high- $z$   
supernova observations*, submitted to A&A (2002).
- IX.** Amanullah, R., Mörtsell, E., & Goobar, A.,  
*Correcting for lensing bias in the Hubble diagram*,  
arXiv:astro-ph/0204280 (2002).

## Acknowledgements

It is a pleasure to acknowledge the influence of Lars Bergström and Ariel Goobar during the years of work in writing this thesis. A small indication of the magnitude of their contribution is their frequent occurrence in the authorlists of the accompanying papers. Apart from this, they have been extremely generous in areas as diverse as providing creative freedom in choosing research projects and providing funds for travelling.

Christofer Gunnarsson, Michael Gustafsson, Martin Eriksson and Mia Schelke deserve special thanks for interesting discussions not necessarily limited to the field of physics. The same goes for my friends in the supernova room: Serena Nobili, Gabriele Garavini, Rahman Amanullah and Gaston Folatelli.

I would also like to thank Martin Goliath with whom I did my first work as a PhD student.

## Acronyms

**Note on units:** Except in the introductory chapters, we use geometrised units, that is,  $G_N = c = 1$ , where  $G_N$  is the Newtonian gravitational constant and  $c$  is the velocity of light in vacuum.

CMBR	Cosmic microwave background radiation
DM	Dark matter
DR	Dyer-Roeder
FL	Friedmann-Lemaître
GR	General (theory of) relativity
MACHO	Massive astrophysical compact halo object
NFW	Navarro-Frenk-White
pdf	probability distribution function
RW	Robertson-Walker
SIS	Singular isothermal sphere
SN	Supernova
SR	Special (theory of) relativity
WIMP	Weakly interacting massive particle

# Contents

<b>1 Laymen/Lekmän</b>	<b>1</b>
Introduction . . . . .	1
Science . . . . .	2
Large numbers and large distances . . . . .	3
A universe of galaxies . . . . .	3
A brief history of the universe . . . . .	4
The fate and weight of our universe . . . . .	5
What happens to the light? . . . . .	6
Gravitational lensing . . . . .	6
Dust . . . . .	7
Disappearing light . . . . .	7
Summary . . . . .	8
Introduktion . . . . .	9
Vetenskap . . . . .	10
Stora tal och stora avstånd . . . . .	10
Ett universum av galaxer . . . . .	11
Universum; en kort historik . . . . .	12
Universums vikt och öde . . . . .	12
Vad händer med ljuset? . . . . .	14
Gravitationslinser . . . . .	14
Stoft . . . . .	15
Försvinnande ljud . . . . .	15
Sammanfattning . . . . .	16
<b>2 Introduction</b>	<b>17</b>
<b>3 Cosmology</b>	<b>19</b>
3.1 Introduction . . . . .	19

3.2	General relativity . . . . .	19
	Special relativity . . . . .	20
	The principles of equivalence . . . . .	22
	Gravitational time dilation and light deflection . . . . .	23
	Metrics and transformations . . . . .	24
	The geodesic equation . . . . .	25
	The geodesic deviation equation . . . . .	27
	The Einstein equations . . . . .	29
3.3	Cosmological models . . . . .	30
	The energy-momentum tensor . . . . .	30
	The Standard Model . . . . .	31
3.4	Distance relations . . . . .	33
3.5	Dark matter . . . . .	36
<b>4</b>	<b>Determination of cosmological parameters</b>	<b>39</b>
4.1	Introduction . . . . .	39
4.2	Cosmological parameters from Type Ia supernovae . . . . .	41
	The magnitude-redshift relation . . . . .	42
	SNAP . . . . .	43
4.3	Systematic effects . . . . .	45
	SNOOC . . . . .	45
<b>5</b>	<b>Gravitational lensing</b>	<b>47</b>
5.1	Introduction . . . . .	47
5.2	History of gravitational lensing <sup>1</sup> . . . . .	47
5.3	Theory of gravitational lensing . . . . .	48
	The deflection angle . . . . .	49
	The lens equation . . . . .	51
	The magnification factor . . . . .	52
5.4	Is it a good thing? . . . . .	53
	Is it always a good thing? . . . . .	54
5.5	Gravitational lensing in SNOOC . . . . .	54
	Multiple images . . . . .	55
5.6	Results . . . . .	55
<b>6</b>	<b>Dust</b>	<b>65</b>
6.1	Introduction . . . . .	65
6.2	Dust and Type Ia supernovae . . . . .	66
6.3	Dust model . . . . .	67

6.4	Dust in SNOC . . . . .	70
6.5	Results . . . . .	71
<b>7</b>	<b>Photon-axion oscillations</b>	<b>75</b>
7.1	Introduction . . . . .	75
7.2	The axion . . . . .	75
	Axions as dark matter . . . . .	77
7.3	Oscillations . . . . .	78
7.4	Results . . . . .	79
<b>8</b>	<b>Conclusions</b>	<b>83</b>
<b>A</b>	<b>Gravitational lensing in Newtonian gravity</b>	<b>85</b>
<b>B</b>	<b>Derivation of the geodesic deviation</b>	<b>89</b>
	Example: point-mass . . . . .	90
	<b>Summary of papers</b>	<b>97</b>



# Chapter 1

## Laymen/Lekmän

In this chapter, I will give a non-technical introduction to cosmology as well as the original work presented in this thesis. It is mainly intended for readers with little or no background in physics.

### Introduction

This thesis is about our universe and how we can learn more about it. A common misconception is that scientists know most things about our universe already. This is not true. A good example is the question of how much matter there is in the universe and what kind of matter this is. Only in the last couple of years have scientists been able to answer the first of these questions to an accuracy of  $\sim 10\%$ .

The second question has proven to be more difficult to answer. A first guess would be that the universe consists of stars. However, adding up the masses of all stars, we are only able to account for  $\sim 0.3\%$  of all the mass in the universe. There is still the possibility that there is matter of the same variety as in stars that we do not observe since it does not shine as brightly as stars. We can calculate and add the contribution from this kind of matter to the mass of the stars to get  $\sim 3\%$ . We are still 97% short! However, observations indicate that there are huge amounts of a kind of invisible matter in the universe, detectable only through its gravitational effects. Adding this component, often referred to as *dark matter*, we get  $\sim 30\%$ . The problem is that we do not know what kind of matter this is, only that it is very different from the matter we are surrounded by here at earth and the matter in stars. The remaining part,  $\sim 70\%$ , is even more of a mystery. It is also invisible, it seems to

fill all of space, it makes space expand and we have no idea what it is. Though we have no idea what it is, there are plenty suggestions and lots of names attributed to it. Often it is referred to as *dark energy*.

Thus, the situation is the following; we think we know how much matter there is in the universe but the larger the fraction, the stranger the kind of matter and the less we know of the nature of the matter component.

## Science

There are different ways to describe something like our universe. Here we will use the method of science which can be very briefly described as follows:

We construct a mathematical model to describe the object or some specific aspects of the object. We then compare the behaviour of the model with observations of the object and fine-tune the model in order to get the highest degree of similarity between the model and the object. This process continues until we cannot reach the desired level of similarity anymore. We then need a new model describing the aspects of the object which the old model could not describe satisfactory. How do we know when we have found the true model? We don't! They are just models describing different aspects of our reality and the relevant question to ask is how well it accomplishes this task. Then why do we bother? In fact, this is just the reason why we bother. The purpose of our model-building is to create models that are simple, yet able to describe different physical phenomena with high enough accuracy for the purpose at hand.

Imagine that we want to model a house. For a lot of purposes, a very convenient model is a simple drawing, just because of the simplicity. Of course, we could build a copy of the house, in scale, and in this way create a very detailed model but this would not be very useful since we then might as well look at the original house. In order to be useful, a model need to be convenient! So why mathematics? Simply because it is usually the easiest way to describe physical phenomena in a convenient way.

In the following I will try to explain some things we know about our universe, in the sense that we have very useful models for its behaviour, as well as what we try to learn.

## Large numbers and large distances

Since our universe is very big, and very old and very much of everything, we often have to use very large numbers when trying to describe it. Instead of writing, e.g., 1000, one therefore writes  $10^3$  where the superscript tells us how many zeros we want. It will turn out to be very convenient to write  $10^{23}$  instead of 100 000 000 000 000 000 000 000.

Also, the distance-measures we use in everyday life, such as metres and kilometers, are not well-suited to measure distances in our universe; they are too small. Instead, one uses the distance travelled by light during certain amounts of time. The velocity of light is 300 000 km/s ( $\sim 10^9$  km/h). That is, in one second light travels a distance of 300 000 km (more than seven turns around the earth), or one *light-second*. One light-second might seem like a long enough distance-measure, but it's not. Instead one often uses light-years, i.e., the distance light travels in one year. Since there are more than 30 million seconds in a year, one light-year is approximately  $10^{13}$  km. This is an incomprehensibly long distance, but since the universe is incomprehensibly large, this is what we have to use.

## A universe of galaxies

We live on planet earth that revolves around the sun – a very ordinary star. Stars are not randomly scattered throughout the universe, but rather gathered in galaxies. Looking at the night-sky, almost every object you see is another star in our galaxy; the Milky Way. There are approximately 100 billion stars in the Milky Way. It takes eight minutes for light from the sun to reach the earth, so we say that the sun is eight light-minutes away. The next nearest star lies at a distance of four light-years. This means that the light we see from that star have been travelling through space four years before it reaches us. What we see is what the star looked like four years ago. All the other 100 billion stars in our galaxy are spread over a distance of 100 000 light-years.

There are at least as many galaxies in the universe as there are stars in our galaxy. Our nearest galaxy neighbour, the Andromeda galaxy, lies at a distance of 2 million light-years. Still, it can be seen with the naked eye. If you find it on the night-sky, remember that the light you see was emitted 2 million years ago; you are actually looking back in time. The furthest galaxies we can observe today, with the aid of powerful telescopes,

lie at a distance of 10 billion light-years.

We do not know just how large the universe is. It might be of infinite extent, or it might have a finite size. Either way, we believe that it has no boundary. It is very hard to imagine anything of finite extent without any boundaries, but the following example might be of some help.

Imagine an ant confined to live its life on the surface of a balloon. Imagine also that this ant has no perception of height. Basically, it can only perceive the two dimensions on the surface of the balloon, which constitutes the ant's universe. This two-dimensional world has a finite extent (the area of the balloon) but no boundary. The same may be true for our three-dimensional universe, even though it is hard to visualise in the same way.

## A brief history of the universe

So, the universe is big, and it's getting bigger all the time. We know that, because when we look at galaxies around us, they are all moving away from us, the further away they are, the faster they are moving.<sup>1</sup> This means that the universe must have been smaller before. Some 15 billion years ago, the universe was so small that the matter in the universe had to be crammed to such an extent that we do not even know how to describe it. At least we know that at some point, the universe started to expand. We call this the *big bang* and we count the age of our universe from this; it is the birth of our universe as we know it.

To understand what happened next, we need to understand gravity. It is gravity that keeps us to the earth's surface. The reason we don't fall off the earth is that the force of gravity attracts matter to other matter, in this case, the earth and our bodies. This is also the reason why matter in the universe is not spread out evenly. In the early universe, matter was indeed spread rather smoothly. However, it was not perfectly smooth, and thus regions which were a little more dense started to attract matter from regions a little less dense, making dense regions denser and less dense regions even less dense. This is the process from which galaxies, stars and planets formed, including the Milky Way, the sun and the earth.

---

<sup>1</sup>The ant living on the surface of a balloon will perceive the same effect if the balloon is inflated.

## The fate and weight of our universe

Will the universe expand forever? It depends upon the amount of matter and energy in the universe. If the universe is very dense, because gravity attracts matter to matter, the universe will be attracted to itself to such an extent that it will gradually halt the expansion and eventually start to contract. If the universe is less dense, the expansion will slow down, but the attraction will not be strong enough to reverse the expansion and the universe will grow larger and larger forever. If there would be no matter whatsoever, the expansion velocity would be constant.

Needless to say, it is not an easy task to determine the density of the universe. We cannot do it by actually weighing it, but it turns out that since more matter means that the expansion of the universe slows down, we can estimate the amount of matter in the universe by measuring the change in the expansion rate. Remember that because of the expansion of the universe, the further away an object is, the faster it will move away from us. Also, the further away an object is, the longer the light from it will have travelled through space. This means that when we measure the expansion velocity of an object at a distance of one million light-years, we really measure the expansion rate of the universe as it was one million years ago. Therefore, by observing recession velocities for different distances, we can measure the change in the expansion velocity of the universe.

How to measure these great distances? Imagine that you look into an ordinary 60 W light-bulb. The further away it is, the weaker the light. By measuring the amount of light you receive from the light-bulb, you can estimate the distance to it. Of course, you have to be sure that it really is a 60 W light-bulb, otherwise you might confuse a nearby 25 W bulb with a further away 60 W bulb. What we need is a very strong source, so that we can see it from very far, with known strength so that we know just *how* far away it is. Fortunately, nature has provided us with such an object; a *supernova*. Supernovae are believed to be exploding stars, and during a couple of weeks, they shine as bright as 100 billion stars or  $10^{34}$  60 W light-bulbs.

So, by determining the distances to supernovae by measuring how bright they are, and compare with their recession velocities, we can determine whether the expansion velocity is constant or if it is slowing down. The results from these measurements are really quite extraordinary. The expansion of the universe seems to be accelerating. Remember that an

empty universe would expand with constant velocity, and that the effect of matter (and we know that there is at least *some* matter in the universe) is to slow down the expansion, due to the force of gravity.

To explain an accelerated expansion of the universe, we need something to drive the expansion and counteract the effects of gravity. This can, e.g., be accomplished by assuming that there is energy in empty space, so-called *vacuum energy*. If there is such a thing, the universe would gain energy by expanding since more space means more energy. Even though it may seem strange that empty space could contain energy, it is still one of the best explanation of an accelerating expansion of the universe yet proposed.

## What happens to the light?

When trying to understand our universe, we look around us using very powerful telescopes. What we look at is the light from distant sources that has travelled through the universe and finally reached us here at earth. Observations of far-away supernovae are very sensitive and we need to make sure that we understand what happens to the light on the way from the supernovae to the earth. Specifically, since we measure the distance to supernovae by measuring luminosities, any effect that will have an effect on the luminosity of a supernova can induce an error in the distance determination. In this thesis, we will look at three different effects capable of altering observed luminosities; gravitational lensing, dust absorption and the conversion of light into other types of particles.

In order to investigate these effects, we have made a computer programme that simulates light from supernovae, travelling through a universe filled with galaxies and dust and other stuff and ultimately reaching us at the earth. Whereas this light-journey takes a billion years in reality, it only takes a second in the computer making it possible to investigate a lot of different effects on a large number of supernovae. The computer code is described in **Paper VIII**.

## Gravitational lensing

We all know that ordinary lenses, like the one used in spectacles and binoculars, are able to magnify light. The amount of magnification depends (among other things) on the form of the lens. Not only ordinary lenses are able to magnify light; very massive objects like galaxies can

have the same effect. This is due to the gravitation from the object, and this kind of lenses are therefore called *gravitational lenses*. The more massive the object, the stronger the gravitational force and the greater the magnification. As for ordinary lenses, the magnification will also depend on the form of the galaxies. Since the universe is full of galaxies, light from a very distant supernova might happen to pass nearby a galaxy on the way to us. If it is magnified, we might be fooled that the supernova is closer than it really is. If light travels through space far away from all galaxies, the supernova will look weaker and further away.

In **Paper I-V** and **IX**, these effects are investigated and it is suggested how this might be corrected for. Also, it is shown that one can in fact use this effect in order to investigate how matter is distributed in the universe.

## Dust

A very simple explanation for something to look weaker than expected is that the light is blocked by something. This something could, e.g., be dust between the source of light and the observer. Looking at the night-sky, one can see dark regions across the Milky Way. These dark patches were once attributed to a deficiency of stars, but are now known to be regions where the background stars are obscured by dust.

Since the effect of an accelerating universe is to make far-away supernovae appear weaker than in a non-accelerating universe, dust has been proposed as an alternative explanation. Since dust not only makes sources look weaker but also redder, we know that there are dust in some galaxies, e.g., our own. In order to mimic the effects of a dark energy component permeating all through space however, we need dust to be distributed evenly. We also need the dust to cause a very small amount of reddening since such an effect would have been observed for far-away sources. In **Paper VI**, we have shown how it is possible to detect the presence of a homogeneous dust density through the small amount of reddening there always is and thereby be able to include the effect when measuring distances to supernovae.

## Disappearing light

Light consists of small particles called *photons*. It is a well known fact that some particles can turn into other types of particles. If some photons

would convert when travelling between a supernova and us, then the supernova will appear dimmer. Effectively, we lose some of the light, an effect very similar to the dust dimming discussed in the previous section.

It has been proposed that the photon might turn into a particle called the axion and then back and forth between the axion and the photon. This mechanism is called *photon-axion oscillations*. The axion is a hypothetical particle originally introduced for very theoretical reasons in the field of particle physics. It has attracted a lot of interest also in cosmology since it's possible that it could be the missing dark matter discussed in the introduction. In this thesis, we investigate the other effect of cosmological importance, namely that photons may turn into axions and thus make supernovae look dimmer. In that respect, axions could very well give an effect very similar to that of the second big mystery in the universe; the dark energy.

In **Paper VII**, we have made simulations in order to predict what the effect of these oscillations could be. We found that the effect will be very different for different photon energies. This implies that we would see very different amounts of light at different energies when we look at far-away objects. This effect is probably not seen, and therefore photon-axion oscillations, if they exist, only is a small effect.

## Summary

The universe is expanding ever since the big bang approximately 15 billion years ago. It is possible to infer the change in the expansion rate by measuring distances and recession velocities of supernovae – exploding stars. The distances are calculated from the observed luminosities of the supernovae; the more luminous it is, the closer it is and vice versa. In order to estimate distances accurately, it is important to understand any alternative mechanisms that can alter the luminosities.

In this thesis, we study three different mechanisms capable of doing this by affecting the light on its way between the supernovae and the observer at earth; focusing of light by gravitational lenses, absorption of light by dust and the possibility that the light is converted to other particles. Even though each of these effects potentially is very important, the current interpretation of the supernova data that the expansion of the universe is accelerating is not severely challenged. This acceleration can, e.g., be driven by a very large fraction of the energy in the universe to be in the form of vacuum energy, i.e., energy in empty space.

I detta kapitel kommer jag att ge en icke-teknisk introduktion till kosmologi samt till den forskning som presenteras i avhandlingen. Det är i första hand avsett för läsare med inga eller mycket begränsade förkunskaper i fysik.

## Introduktion

Denna avhandling handlar om vårt universum och hur vi kan lära oss mer om det. En vanlig missuppfattning är att vetenskapsmän och -kvinnor redan vet allt som finns att veta om universum. Så är inte fallet. Ett bra exempel är frågan om hur mycket materia det finns i universum och av vilket slag den är. Det är bara de senaste åren som vetenskapen kunnat ge ett svar på den första frågan till en noggrannhet av  $\sim 10\%$ .

Den andra frågan har visat sig vara än svårare att besvara. En första gissning är att universum till största delen består av stjärnor men om vi adderar massan hos alla stjärnor så kommer vi bara upp till  $\sim 0.3\%$  av universums totala massa. Det finns fortfarande en möjlighet att det finns materia av samma slag som i stjärnor men som vi inte kan se eftersom den inte lyser lika starkt. Om vi beräknar denna massa och lägger till massan hos alla stjärnor kommer vi upp till  $\sim 3\%$ . Det fattas fortfarande 97%!

Det finns observationer som visar på stora mängder av något slags osynlig materia som bara gör sig påmind genom de gravitationskrafter den orsakar. Om vi adderar även denna komponent, ofta kallad *mörk materia*, kommer vi upp till  $\sim 30\%$ . Problemet är att vi inte vet vad för slags materia detta är, bara att den är helt annorlunda mot all materia vi är omgivna av här på jorden och materien i stjärnor. Den återstående delen,  $\sim 70\%$ , är än mer av ett mysterium. Den är också helt osynlig, den verkar fylla hela rymden, den får rymden att expandera och vi har ingen aning om vad den är för något. Trots att vi egentligen inte vet något om den, finns det gott om förslag på vad den kan vara för något och vad den ska kallas. En vanlig benämning är *mörk energi*.

Situationen kan alltså sammanfattas på följande sätt; vi vet hur mycket materia det finns i universum men ju mer det finns av en viss komponent, desto mindre vet vi om den.

## Vetenskap

Det finns olika sätt att beskriva till exempel vårt universum. Häданefter kommer jag att använda mig av den vetenskapliga metoden, vilken kort kan sammanfattas på följande sätt:

Först konstruerar vi en matematisk modell för att beskriva objektet eller vissa specifika aspekter av det. Sedan jämför vi vår modell med observationer av objektet och anpassar modellen tills vi nått högsta möjliga grad av överensstämmelse. Denna process fortgår tills vi inte längre kan nå önskad överensstämmelse och det krävs en ny modell för att beskriva de aspekter av objektet som den gamla modellen misslyckades med att beskriva. Hur vet vi när vi har hittat den sanna modellen? Det vet vi inte! De är endast att betrakta just som modeller vars uppgift är att beskriva vissa valda delar av vår omgivning och den relevanta frågan att ställa sig är snarare hur bra modellen lyckas med dennna uppgift. Varför gör vi oss då detta besvä? Jo, syftet är att skapa modeller som är så enkla som möjligt men som ändå kan beskriva olika fenomen med tillräckligt hög noggrannhet.

Tänk dig att vi vill göra en modell av ett hus. För de flesta syften är en vanlig ritning en mycket bra modell just därför att den är så enkel. Vi skulle naturligtvis kunna bygga en fullskalig kopia av huset och på detta sätt skapa en mycket detaljerad modell men den skulle inte vara särskilt användbar eftersom vi då lika gärna kan studera det ursprungliga huset. En modell måste alltså vara praktisk för att bli användbar.

Varför använder vi då matematiska modeller? Helt enkelt därför att de vanligtvis är det mest praktiska sättet att beskriva fysikaliska fenomen.

Jag ska nu försöka förklara något av det vi vet om universum, i betydelsen att vi har användbara modeller för att beskriva det, samt även diskutera vad vi försöker lära oss mer om.

## Stora tal och stora avstånd

Eftersom universum är väldigt stort och väldigt gammalt och väldigt mycket av allt, krävs det väldigt stora tal för att beskriva det. Istället för att skriva t.ex. 1000, skriver man därför  $10^3$  där exponenten (talet 3) talar om hur många nollor det ska vara. Det har visat sig vara mycket praktiskt att skriva  $10^{23}$  istället för 100 000 000 000 000 000 000.

Avståndsmåtten vi använder till vardags, som meter och kilometer, är inte anpassade till att mäta avstånd i universum; de är helt enkelt alldeles

för små. Istället använder man sträckan som ljus tillryggalägger under vissa tidsrymder. Ljusets hastighet är  $300\,000 \text{ km/s}$  ( $\sim 10^9 \text{ km/h}$ ). Under loppet av en sekund tillryggalägger ljuset alltså  $300\,000 \text{ km}$  (mer än sju varv runt ekvatorn), eller en *ljus-sekund*. En ljus-sekund kan tyckas vara långt nog som avståndsmått, men det är det inte. Istället använder man ljusår; den sträcka ljus hinner färdas under loppet av ett år. Eftersom det går fler än  $30$  miljoner sekunder på ett år så är ett ljusår ungefär  $10^{13} \text{ km}$ . Detta är ett ofattbart stort avstånd, men eftersom universum är ofattbart stort så är det vad som krävs för att beskriva det.

## Ett universum av galaxer

Vi lever på planeten jorden som snurrar runt solen, en ganska ordinär stjärna. Stjärnor är inte slumpröviga utspridda i universum utan samlade i galaxer. Om du tittar på stjärnhimlen är nästan allt du ser stjärnor i vår egen galax; Vintergatan. Det finns ungefär  $100$  miljarder stjärnor i Vintergatan. Det tar åtta minuter för ljus från solen att nå jorden; solen ligger alltså på ett avstånd av åtta ljusminuter. Den näst närmsta stjärnan ligger på ett avstånd av fyra ljusår. Detta betyder att ljuset vi ser från den stjärnan har färdats i fyra år genom rymden innan det når oss. Vad vi ser är alltså hur stjärnan såg ut för fyra år sedan. Alla andra  $100$  miljarder stjärnor i vår galax ligger utspridda över ett avstånd av  $100\,000$  ljusår.

Det finns åtminstone lika många galaxer i universum som det finns stjärnor i vår galax. Vår närmsta galaxgranne, Andromedagalaxen, befinner sig på ett avstånd av  $2$  miljoner ljusår. Trots detta kan vi se den med blotta ögat. Om du hittar den på stjärnhimlen, betänk att ljuset du ser lämnade Andromedagalaxen för  $2$  miljoner år sedan; du ser bakåt i tiden! Med hjälp av kraftfulla teleskop kan vi idag observera galaxer på ett avstånd av  $10$  miljarder ljusår.

Vi vet inte riktigt hur stort universum är. Oavsett om det är oändligt stort eller har ändlig storlek så tror vi att det inte har någon gräns. Det är naturligtvis svårt att tänka sig något med ändlig storlek men utan gräns men följande exempel kan kanske vara till viss hjälp.

Tänk dig en myra som är hävdat att leva sitt liv på ytan av en ballong. Tänk dig också att den inte kan uppfatta begreppet höjd utan endast de två dimensionerna på ytan av ballongen som utgör myrans universum. Denna tvådimensionella värld har ändlig storlek (ytan på ballongen) men ingen gräns. Samma förhållande kan tänkas gälla i vår

tredimensionella värld även om det är svårt att visualisera på samma sätt.

## Universum; en kort historik

Inte nog med att universum är väldigt stort, det blir bara större och större hela tiden. Det vet vi eftersom när vi tittar på andra galaxer så rör de sig bort från oss, ju längre bort de ligger, desto snabbare rör de sig.<sup>2</sup> Det betyder att universum måste ha varit mindre förut. För ungefär 15 miljarder år sedan var universum så litet att materien var så tätt sammanpackad att vi inte kan beskriva den med dagens fysikaliska teorier. Vi vet åtminstone att vid någon tidpunkt började universum att expandera. Vi kallar detta *big bang* och räknar universums ålder från denna tidpunkt.

För att kunna förstå vad som hände sedan måste vi förstå hur gravitationen verkar. Det är gravitationen som hindrar oss från att trilla av jorden. Anledningen till att vi håller oss kvar på jordens yta är att gravitationskraften verkar som en attraktionskraft mellan materia och annan materia, i detta fall jorden och våra kroppar. Den är också orsaken till att materien i universum inte är jämnt utspridd. I det tidiga universum var materien relativt jämnt, men inte helt perfekt, utspridd. Regioner som var lite tätare började dra till sig materia från områden som var lite mindre tätta. På detta sätt blev tätta regioner ännu tätare och mindre tätta regioner ännu mindre tätta. Det är genom denna typ av process som galaxer, stjärnor och planeter bildas, som till exempel Vintergatan, solen och planeten jorden.

## Universums vikt och öde

Kommer universum att fortsätta expandera för evigt? Det beror på mängden materia och energi i universum. Eftersom gravitationen verkar som en attraktionskraft mellan materia så kommer universum, om det innehåller tillräckligt mycket materia, att vara attraherat av sig själv i så hög grad att expansionen avtar och det istället börjar att dra ihop sig. Om universum innehåller mindre materia kommer attraktionen inte att vara stark nog att vända på expansionen och universum kommer att bli

---

<sup>2</sup>Myran som lever på ytan av en ballong uppfattar samma effekt när ballongen blåses upp till större storlek.

---

större och större i all evighet. Om det inte fanns någon materia alls skulle expansionshastigheten vara oförändrad.

Det är naturligtvis ingen lätt uppgift att bestämma mängden materia i universum. Vi kan inte göra det genom att väga det, men det visar sig att eftersom en stor mängd materia gör att expansionshastigheten avtar kan vi uppskatta mängden materia genom att mäta hur expansionshastigheten ändras med tiden. Kom ihåg att universums expansion medför att ju längre bort en galax befinner sig, desto snabbare rör den sig bort ifrån oss. Minns även att ljuset från en galax har färdats längre tid genom rymden ju längre bort galaxen ligger. Det innebär att när vi mäter hastigheten hos ett objekt som befinner sig på ett avstånd av en miljard ljusår, mäter vi den hastighet som objektet rörde sig bort ifrån oss med för en miljard år sedan. På detta sätt är det möjligt att se hur expansionshastigheten hos universum ändras genom att observera hastigheter för objekt som befinner sig på olika avstånd från jorden.

Hur är det då möjligt att mäta dessa enorma avstånd? Tänk dig att du betraktar en helt vanlig 60 W glödlampa. Eftersom ljuset blir svagare ju längre bort den befinner sig kan vi uppskatta avståndet till den genom att mäta ljusstyrkan. Naturligtvis måste vi vara säkra på att det verkligen är en 60 W glödlampa, annars kan vi ta fel på en närliggande 25 W lampa och en 60 W lampa som ligger längre bort. Vad vi behöver är alltså en mycket stark ljuskälla, så att vi kan se den på långt håll, med känd effekt, så att vi kan bestämma precis *hur* långt bort den befinner sig. Som tur är finns det just ett sådant objekt; en supernova. Supernovor är exploderande stjärnor och under loppet av ett par veckor lyser de lika starkt som 100 miljarder stjärnor eller  $10^{34}$  60 W glödlampor.

Genom att bestämma avståndet till supernovor med hjälp av hur ljusstarka de ser ut och jämföra deras hastigheter kan vi alltså avgöra om expansionen har konstant hastighet eller om den saktar ned. Resultatet av dessa mätningar är tämligen uppseendeväckande; expansionshastigheten verkar accelerera. Minns att ett tomt universum expanderar med konstant hastighet och att effekten av materia (och vi vet att det finns åtminstone *lite* materia i universum) är att sakta ned expansionen med hjälp av gravitationskraften.

För att kunna förklara en accelererande expansion av universum behöver vi något som driver på expansionen och motverkar gravitationskraften. Detta kan till exempel åstadkommas genom att anta att att det finns mörk energi i tomma rymden, ibland kallad vakuumenergi. Om det

finns energi i vakuum tjänar universum energi på att expandera eftersom mer rymd innehåller mer energi. Även om det kan verka konstigt att det kan finnas energi i vakuum är det ändå en av de bästa förslagen till förklaring av universums accelererande expansion.

## Vad händer med ljuset?

När vi försöker förstå universum ser vi oss omkring med hjälp av kraftfulla teleskop. Vad vi ser är ljus som färdats genom rymden från avlägsna källor och slutligen nått oss här på jorden. Observationer av avlägsna supernovor är mycket känsliga och vi måste försäkra oss om att vi förstår vad som händer med ljuset på vägen mellan supernovan och oss. Eftersom vi bestämmer avståndet till supernovor genom att mäta ljusstyrkan kommer varje sak som förändrar ljusstyrkan att ge ett fel i avståndsbedömningen. I min avhandling studerar jag tre olika saker som kan göra just detta; gravitationell linsning, stoft och möjligheten att ljus omvandlas till andra partiklar.

I syfte att utreda dessa effekter har vi utvecklat ett datorprogram som simulerar ljus ifrån supernovor som färdas genom ett universum fyllt av galaxer och stoft och annat för att till sist nå oss här på jorden. Denna resa tar miljarder år i verkligheten men i datorn tar det bara någon sekund vilket innebär att vi kan titta på många olika effekter och många supernovor. Datorprogrammet är beskrivet i **Paper VIII**.

## Gravitationslinser

Vi vet att vanliga linser som de i glasögon och kikare kan fokusera och förstärka ljus. Graden av förstärkning beror (bland annat) på linsens form. Det är inte bara vanliga linser som har förmågan att förstärka ljus; väldigt massiva objekt som galaxer kan ha samma effekt. Eftersom detta är en effekt av gravitationen från objektet kallas dessa linser för *gravitationslinser*. Ju mer massivt ett objekt är, ju starkare är gravitationskraften och ju större blir förstärkningen. Precis som för vanliga linser beror graden av förstärkning även på galaxens form. Eftersom universum är fyllt av galaxer kan det hända att ljuset från en avlägsen supernova passerar nära en galax på vägen till oss. Om ljuset förstärks kan vi luras att tro att supernovan ligger närmare än vad den egentligen gör. Om ljuset från supernovan färdas långt ifrån alla galaxer kommer ljuset att vara svagare och supernovan ge intryck av att ligga längre bort.

I Paper I-V och IX studerar vi dessa effekter och föreslår hur man kan korrigera för dem. Vi visar också hur man kan använda linseffekten för att lära sig något om hur materien är utspridd i universum.

## Stoft

En enkel förklaring till att något ser ut att vara ljussvagare än förväntat är att något blockerar ljuset. Detta något kan till exempel vara stoft som befinner sig mellan ljuskällan och observatören. När man tittar på stjärnhimlen kan man se mörka stråk genom Vintergatan. Dessa mörka områden trodde man först var en följd av att där inte fanns några stjärnor men nu vet vi att det är områden där ljuset från stjärnorna blockeras av stoft.

Eftersom en av följderna av ett accelererande universum är att avlägsna supernovor ser ljussvagare ut än i ett icke-accelererande universum, har stoft föreslagits som en alternativ förklaring. Vi vet att det finns stoft i vissa galaxer, inklusive vår egen, eftersom stoft inte bara får ljuskällor att se svagare ut utan även rödare. För att ge samma synbara effekt som vakuumenergi vilken fyller hela rymden krävs det dock att stoftet är väldigt jämnt utspritt. Vi kräver även att stoftet inte gör att saker ser alltför röda ut eftersom detta i sådana fall redan skulle ha observerats för avlägsna källor. I Paper VI har vi visat hur det är möjligt att påvisa förekomsten av väldigt jämnt utspritt stoft just genom att titta på hur supernovor skulle komma att se lite rödare ut än normalt. Därigenom kan vi ta hänsyn till effekten när vi mäter avståndet till supernovor.

## Försvinnande ljud

Ljud består av små partiklar som kallas *fotoner*. Det är ett välkänt faktum att vissa partiklar kan förvandlas till andra slags partiklar. Om en del fotoner förvandlas under färden mellan supernovan och oss kommer supernovan att se ljussvagare ut. Vi förlorar helt enkelt en del av ljuset, en effekt som påminner om den orsakad av stoft som berördes i förra avsnittet.

Det har föreslagits att fotonen kan förvandlas till en partikel som kallas för en axion och sedan fram och tillbaka mellan de två partikelslagen. Denna mekanism kallas för *foton-axion oscillationer*. Axionen är en hypotetisk partikel som uppfanns av teoretiska skäl inom partikelfysiken. Den har ådragit sig stort intresse även inom kosmologin eftersom den

möjligtvis skulle kunna utgöra den mörka materia som diskuterades i introduktionen. I avhandlingen undersöker vi en annan effekt av betydelse inom kosmologin, nämligen att fotoner kan omvandlas till axioner och därigenom få supernovor att se ljussvagare ut. I detta avseende kan axioner ha en synbar effekt väldigt lik den orsakad av det andra stora mysteriet i universum; vakuumenergin.

I **Paper VII** har vi simulerat effekten av denna typ av oscillationer. Resultatet är att effekten är väldigt olika för olika fotonenergor. Det betyder att vi skulle se väldigt olika mycket ljus vid olika energier när vi observerar avlägsna objekt. Denna effekt har antagligen inte observerats, och därfor är foton-axion oscillationer, om de existerar, endast en mycket svag effekt.

## Sammanfattning

Universum har expanderat ända sedan big bang för ungefär 15 miljarder år sedan. Det är möjligt att mäta hur universums expansionshastighet ändras genom att mäta med vilken hastighet supernovor – exploderande stjärnor – på olika avstånd rör sig bort ifrån oss. Avstånden bestäms genom att mäta ljusstyrkan; en närliggande supernova lyser starkare än en som ligger längre bort. För att kunna göra en korrekt avståndsbedömning är de viktigt att förstå alla övriga mekanismer som kan påverka ljusstyrkan.

I den här avhandlingen studeras tre olika mekanismer som kan påverka ljuset under dess färd mellan supernovan och jorden; förstärkning av ljuset av gravitationslinser, blockering av ljuset av stoft samt möjligheten att ljuspartiklar, fotoner, omvandlas till andra partiklar. Även om alla dessa mekanismer potentiellt är väldigt viktiga, är fortfarande den gängse tolkningen av supernova-observationerna att universums expansion accelererar. Denna acceleration kan till exempel vara en följd av att en stor mängd av universums energi är i form av vakuumenergi, alltså energi i tomma rymden.

# Chapter 2

## Introduction

The universe is found to have been accelerating for the last 6 billion years! This discovery was the "Science breakthrough of the year 1998" according to Science Magazine [32].

This is a remarkable discovery indeed. First of all because almost everything we know about about the universe, we know from tiny amounts of light reaching us at earth from sources so distant we can hardly imagine it. To be able to foretell the ultimate fate of the universe from this scarce information is a huge accomplishment. Second, because the fact that the expansion of the universe is accelerating is remarkable in itself.

That the universe is expanding has been known since Hubble's discovery of the distance-redshift relation. Since an empty expanding universe would continue to expand with the same velocity, it was generally believed that the universe would decelerate due to the opposing force of gravity, trying to pull matter closer to other matter in the universe. In order to have an accelerating universe, we need a significant part of the energy density to be in some so far unknown form with a number of strange properties. Since this can be regarded a big conceptual step to take, we need to take all possible alternative explanations into account, as well as to investigate any independent evidence carefully.

The supernova (SN) evidence for an accelerating universe is based on the same method as used by Hubble to prove that the universe is expanding, namely by measuring recession velocities as a function of distance. Since the velocity of light is finite, we can measure the expansion velocity at different epochs by measuring it at different distances. To determine the recession velocity from redshifting of spectral lines is a fairly straight-

forward procedure whereas the determination of cosmological distances is a very complex problem. Since different Type Ia SNe have very similar luminosities, we can use the fact that the further away an object is, the fainter it will appear in order to determine distances. An accelerating universe will have the effect of making objects with a certain redshift look fainter than in a universe with constant expansion. This effect has also been observed by two independent research groups [26, 30].

There is independent evidence supporting the interpretation of the SN data in terms of an accelerating universe, most notable from measurements of the cosmic microwave background radiation (CMBR) combined with large scale structure observations. Still, it is of great importance to investigate any source of possible systematic errors in the SN data itself. In this thesis, we investigate three different mechanisms capable of affecting the observed luminosities of SNe with main emphasis on the possible systematic bias in the cosmological parameter estimation, namely gravitational lensing, dust extinction and the, perhaps exotic, possibility of photon-axion oscillations. We also show how one can use SN data to obtain information on the distribution of dark matter (DM) and the properties and abundances of intergalactic dust.

In Ch. 3 and 4 we give a short introduction to cosmology and the determination of cosmological parameters. In the subsequent chapters, the effects of gravitational lensing, dust extinction and photon-axion oscillations are studied. These effects have been proposed as possible sources of systematic error in the determination of cosmological parameters from SNe. There have even been claims that the latter two effects could be responsible for almost all the dimming usually attributed to a cosmological constant. Since, as noted, there are other measurements supporting the notion of a significant dark energy component, it is generally believed that these effects are not responsible for all the dimming. However, they could still introduce a severe bias in the Hubble diagram and if we want to be able to determine cosmological parameters with high accuracy, we need to control any systematic effects.

In short, these effects are capable of affecting any observations of astronomical sources at cosmological distances. In that respect, the main question of this thesis is: What happens to light travelling through our universe?

# Chapter 3

# Cosmology

In this chapter, some basic facts about cosmology is reviewed with particular attention given to the theory needed for the subsequent chapters, e.g., cosmological parameters, distance relations and dark matter.

## 3.1 Introduction

Cosmology is the study of the nature and evolution of our universe. As in other sciences, the goal is to construct models that, while being as simple and comprehensive as possible, are able to explain very diverse and complex phenomena. The observational information that the theoretical models are compared with consists of electromagnetic radiation and particles arriving to the earth from different astrophysical sources.

During the last couple of years, the amount of observational information has increased rapidly, triggering a wealth of new interpretations and theoretical models. Even so, arguably the most important theoretical model in cosmology and one that has survived the test of time since its birth in 1916 is Einstein's general theory of relativity (GR). We therefore begin this short summary of modern cosmology by devoting a couple of pages to the basics of GR.

## 3.2 General relativity

We know of four fundamental physical forces governing the behaviour of objects in the physical world; the strong force, the weak force, the electromagnetic force and the force of gravity. Although extremely weak

on small scales, on the very large scales of our universe, gravity is the most important force. This is due to the fact that the range of the force is unlimited, that it is always attractive for matter (if a cosmological constant exists, there may also be a repulsive part) and that it is the only force that acts between all kinds of matter.

The first coherent theory of gravity was formulated in 1687 by Newton in his *Principia* and is still used as an excellent approximation in a multitude of cases. However, when we want to describe very strong gravitational fields or the large scale behaviour of the universe, we need to use GR. As the name suggests, the general theory of relativity is a generalisation of another theory, the special theory of relativity.

## Special relativity

Einstein developed the special theory of relativity (SR) from the seemingly harmless postulate that all inertial frames should be equivalent, i.e., that the laws of physics should have the same form in all inertial frames. An inertial frame is defined as a system where a free particle, that is, a particle not subject to any force, remains at rest or in steady, rectilinear motion. Assuming further that Maxwell's equations for the electromagnetic field are correct, then there follows that the velocity of light in vacuum,  $c$ , is a universal constant, which has the same value in all inertial frames (in this thesis, we set  $c = 1$ ). A consequence of this is that there can exist no absolute, universal time as in Newton's theory of gravity. Thus, an important concept in SR is *spacetime* where the three dimensions of space and the dimension of time are linked together.

We parametrise spacetime by introducing coordinates  $x^0 = t, x^1 = x, x^2 = y, x^3 = z$ , with respect to some inertial system  $K$ . These four components constitute a *four-vector*,

$$x^\alpha = (t, x^i) = (t, \mathbf{r}). \quad (3.1)$$

Following convention, greek indices like  $\alpha$ , run from 0 to 3 and latin indices, like  $i$ , run from 1 to 3. In the same way, we can introduce spacetime coordinates  $x'^\alpha$  for any inertial frame  $K'$ .

The distance squared between two neighbouring points in three-dimensional Euclidean space is

$$ds^2 = (dx^1)^2 + (dx^2)^2 + (dx^3)^2$$

$$\begin{aligned}
&= \begin{pmatrix} dx^1 \\ dx^2 \\ dx^3 \end{pmatrix}^T \begin{pmatrix} 1 & 0 & 0 \\ 0 & 1 & 0 \\ 0 & 0 & 1 \end{pmatrix} \begin{pmatrix} dx^1 \\ dx^2 \\ dx^3 \end{pmatrix} \\
&= (\mathbf{d}\mathbf{r})^T \mathbf{G}(\mathbf{d}\mathbf{r}). \tag{3.2}
\end{aligned}$$

The  $3 \times 3$  matrix  $\mathbf{G}$  constructs the quadratic form that corresponds to the square of the distance. This matrix is the *metric tensor* in Euclidean space. A tensor is a mapping from a vector to another vector, or, as in the case of the metric tensor  $\mathbf{G}$ , from a vector to a scalar. The metric tensor  $\mathbf{G}$  is constant but in general, a tensor can vary from point to point in spacetime.

We can write the metric equation in a more compact way by introducing the *Einstein summation convention* where an index that is repeated twice is summed over,

$$ds^2 = \sum_{i,j=1}^3 G_{ij} dx^i dx^j =: G_{ij} dx^i dx^j. \tag{3.3}$$

Analogously to distance in the three-dimensional Euclidean space we define the square of an interval,

$$ds^2 := -(dx^0)^2 + (dx^1)^2 + (dx^2)^2 + (dx^3)^2, \tag{3.4}$$

between two events  $x^\alpha$  and  $x^\alpha + dx^\alpha$  in four-dimensional spacetime. The spacetime interval  $ds$  is invariant under transformations from one inertial frame to another, i.e., it has the same value in every inertial frame. As can be seen from Eq. (3.4), the four-dimensional metric tensor for an inertial frame that is the analogue of the three-dimensional metric tensor  $\mathbf{G}$  is

$$\eta_{\alpha\beta} = \begin{pmatrix} -1 & 0 & 0 & 0 \\ 0 & 1 & 0 & 0 \\ 0 & 0 & 1 & 0 \\ 0 & 0 & 0 & 1 \end{pmatrix}. \tag{3.5}$$

This metric is called the Minkowski metric, and spacetime with this metric is called Minkowski space. The identity

$$ds^2 = dt^2 [d\mathbf{r}^2/dt^2 - 1] \tag{3.6}$$

relates the velocity  $d\mathbf{r}/dt$  with the sign of  $ds^2$ :

$$ds^2 > 0 \quad \text{space-like separations}$$

$$\begin{aligned} ds^2 &= 0 && \text{light-like separations} \\ ds^2 &< 0 && \text{time-like separations} \end{aligned}$$

In the next section we will see how Einstein succeeded in generalising special relativity to treat also non-inertial frames (e.g., accelerated frames) and incorporating the effects of gravitation into the theory using the principles of equivalence. In fact, we will learn that dealing with gravitation and accelerated frames is equivalent according to general relativity.

## The principles of equivalence

It is an experimental fact that different bodies placed in the same gravitational field acquire the same acceleration, i.e., the gravitational mass and the inertial mass are equal. This equality is called the *weak equivalence principle*.

Consider two spacecrafts, one standing still on the surface of the earth and one in space, far away from gravitating masses but with a constant acceleration equal to the gravitational acceleration  $g$  at the earth's surface. The equality of gravitational and inertial masses makes it impossible to distinguish between these two situations by performing experiments with falling bodies inside the spacecrafts.<sup>1</sup> Suppose that we perform experiments with freely falling experimental apparatus in both rockets. Since, according to the weak equivalence principle, the situations should be indistinguishable, we postulate that the experimental outcome should be identical, i.e., a reference system falling freely in a homogeneous gravitational field is equivalent to an inertial system. This is the *strong equivalence principle*; the results of all local experiments in a freely falling frame are consistent with the special theory of relativity.

These principles are the postulates of GR and using these we can derive two of its most important results, both of which will be of considerable importance for the theory of gravitational lensing,

- that time runs slower in the presence of a gravitational field, and

---

<sup>1</sup>There is a slight difference. The gravitational field in the rocket standing on the earth's surface will be inhomogeneous due to the fact that it has the earth as its source, see Fig. 3.4. If we restrict ourselves to local experiments, the gravitational field can be regarded as homogeneous and the two situations are indistinguishable in the above sense.

- that the path of a light-ray is bent when traversing a gravitational field.

## Gravitational time dilation and light deflection

Consider an elevator in free fall in, e.g., the earth's gravitational field, starting with zero velocity and with constant acceleration  $g$ , see Fig. 3.1. A clock at the floor of the elevator controls a laser where each light-pulse defines a unit of time as measured at the location of the laser. The pulses are received at a height  $\Delta h$  above the source where the time interval between the arrival of the pulses gives the relation between the pace of time at height  $\Delta h$  and at the floor of the elevator. We know from the strong equivalence principle that light travels with constant velocity  $c = 1$  in a freely falling frame, so that after a time  $\Delta t = \Delta h$  as measured inside the elevator, the light-pulse reaches the observer at height  $\Delta h$ . During this time interval, the elevator has accelerated to a velocity

$$\Delta v = g\Delta t = g\Delta h. \quad (3.7)$$

An outside observer at the same position as the laser but at rest with respect to the earth will measure the pulses at the same frequency as an observer at the floor of the elevator whereas an outside observer at the same position as the receiver will measure the pulses at a frequency which is lower by the relative amount

$$\frac{\Delta\nu}{\nu} = \Delta v = g\Delta h. \quad (3.8)$$

Thus, for observers at rest in the earth's gravitational field, time runs slower at the height of the floor of the elevator than at a height  $\Delta h$  above it by the fractional amount  $g\Delta h$ .<sup>2</sup>

Once again we consider the freely falling elevator, but this time we let an experimentalist shine the laser beam horizontally across the elevator, see Fig. 3.2. For the experimentalist in the freely falling frame (inside the elevator), the light-ray will hit the other wall at the same height as the emitter. The outside observer will see the elevator move downwards a

---

<sup>2</sup>One might argue that this is only a consequence of the specific definition of time used in the example. However, the definition uses the velocity of light which governs the speed of all physical processes, including biological. Thus, the outside observer at the height of the floor of the elevator will in fact grow older slower than the outside observer at the height of receiver.

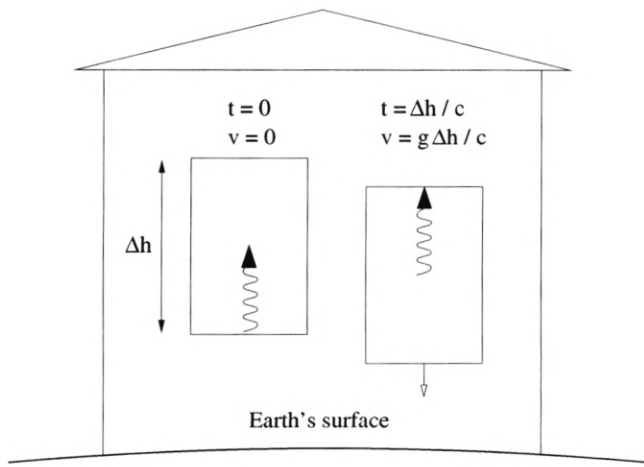


Figure 3.1: Gravitational time dilation in the earth's gravitational field.

small distance before the light-ray hits the wall. Therefore, to the observer in the earth's gravitational field, it seems that the light-ray follows a bent path, i.e., gravity deflects light.

### Metrics and transformations

We now introduce a metric tensor,  $g_{\alpha\beta}(x^0, x^1, x^2, x^3)$ , to give a real number, the square of the distance, between two infinitesimally nearby events. This is the general case of Eq. (3.4) where, in contrast to the Minkowski metric, we allow the metric tensor to vary from point to point. For convenience of abbreviation, we will hereafter suppress its explicit coordinate dependence.

From the strong principle of equivalence, we know that we can always locally find a reference frame  $K_P$  with coordinates  $x^\alpha$  such that

$$g_{\alpha\beta}(P) = \eta_{\alpha\beta} \quad \text{and} \quad (3.9)$$

$$\left. \frac{\partial g_{\alpha\beta}}{\partial x^\mu} \right|_P = 0. \quad (3.10)$$

Here,  $P$  is an arbitrary, given point in spacetime. This is the free fall system at  $P$ , and  $K_P$  is a local inertial frame. Restricting ourselves to small spacetime regions around  $P$ , the coordinate transformation from an arbitrary reference system to a local inertial frame will be linear. If

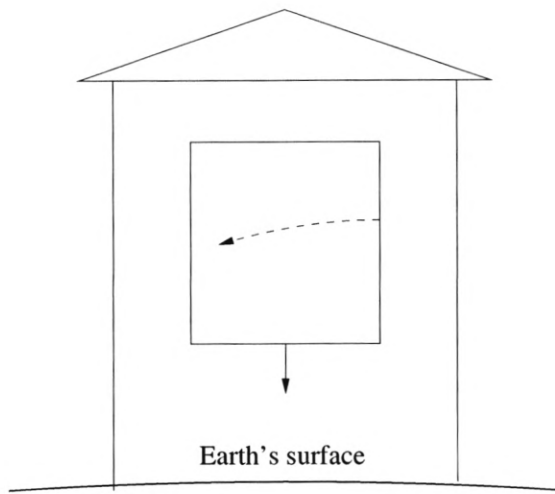


Figure 3.2: Light deflection in the earth's gravitational field. Note that the effect is highly exaggerated.

we denote spacetime coordinates in a local inertial frame with primes, it follows that

$$dx'^\beta = \frac{\partial x'^\beta}{\partial x^\alpha} dx^\alpha, \quad (3.11)$$

where  $x^\alpha$  are coordinates in an arbitrary reference system, e.g., an accelerating frame.

### The geodesic equation

Since the distance between two events on the trajectory of a massive particle is invariant, we can choose to calculate it in the rest frame of the particle which yields

$$ds^2 = g_{\alpha\beta} dx^\alpha dx^\beta = -(dx^0)^2 =: -d\tau^2. \quad (3.12)$$

This defines the invariant parameter  $\tau$ , called *proper time*, as the time measured by a clock following the particle. In a local inertial frame, the proper time  $\tau$  is, in accordance with SR, given by

$$-d\tau^2 = \eta_{\alpha\beta} dx'^\alpha dx'^\beta, \quad (3.13)$$

whereas it in an arbitrary reference system takes the form

$$-d\tau^2 = g_{\alpha\beta} dx^\alpha dx^\beta, \quad (3.14)$$

where, following from Eq. (3.11),

$$g_{\alpha\beta} = \eta_{\mu\nu} \frac{\partial x'^\mu}{\partial x^\alpha} \frac{\partial x'^\nu}{\partial x^\beta}. \quad (3.15)$$

In terms of the free fall coordinates  $x'^\alpha$ , the equation of motion of a free particle is

$$\frac{d^2 x'^\alpha}{d\tau^2} = 0. \quad (3.16)$$

A short calculation involving the chain rule shows that the corresponding expression in terms of the arbitrary coordinates  $x^\alpha$  is

$$\frac{d^2 x^\alpha}{d\tau^2} + \Gamma^\alpha_{\mu\nu} \frac{dx^\mu}{d\tau} \frac{dx^\nu}{d\tau} = 0, \quad (3.17)$$

where

$$\Gamma^\alpha_{\mu\nu} = \frac{\partial x^\alpha}{\partial x'^\sigma} \frac{\partial^2 x'^\sigma}{\partial x^\mu \partial x^\nu}. \quad (3.18)$$

Equation (3.17) is called the *geodesic equation* and  $\Gamma^\alpha_{\mu\nu}$  are the metric connections. Geodesics are curves analogous to straight lines in Euclidean space. The paths of freely falling objects in spacetime are time-like geodesics while light follows light-like geodesics. However, there is no change in proper time along the path of a photon, so  $\tau$  cannot be used as a parameter. Instead, we use a so-called affine parameter  $\lambda$ , so that the analogue of Eq. (3.17) for a photon is

$$\frac{d^2 x^\alpha}{d\lambda^2} + \Gamma^\alpha_{\mu\nu} \frac{dx^\mu}{d\lambda} \frac{dx^\nu}{d\lambda} = 0. \quad (3.19)$$

In moving from the flat spacetime of SR in the local inertial frame to the curved spacetime of GR in the arbitrary frame, we incorporate the effects of gravity, and thus the geodesic equation can be interpreted as a force equation,

$$\frac{d^2 x^\alpha}{d\tau^2} = f^\alpha \quad \text{with} \quad f^\alpha = -\Gamma^\alpha_{\mu\nu} \frac{dx^\mu}{d\tau} \frac{dx^\nu}{d\tau}. \quad (3.20)$$

However, in GR, gravity is not regarded as a force in the conventional sense. Instead, gravitational effects are explained in terms of the curvature of spacetime caused by the presence of matter. Comparing Eq. (3.17) with its free fall analogue Eq. (3.16) it is obvious that the metric connections play an important role in gravitational effects. It can be shown that the  $\Gamma^\alpha_{\mu\nu}$  are entirely built up of the  $g_{\alpha\beta}$  and its first derivatives, justifying the view of gravity as a purely geometrical effect.

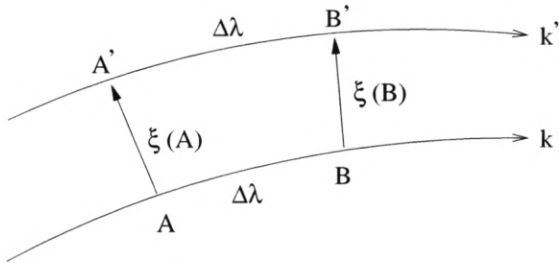


Figure 3.3: Deviation of two initially parallel, infinitesimally separated geodesics.

### The geodesic deviation equation

In curved space, parallel lines when extended do not remain parallel. Consider two geodesics parametrised by the parameter  $\lambda$  that begin parallel, see Fig. 3.3. The geodesics have tangents  $k$  and  $k'$ , and they are connected by a vector  $\xi$  at points at equal intervals of  $\lambda$ . Using a locally inertial frame, the geodesic equation at  $A$  is

$$\frac{d^2x^\alpha}{d\lambda^2}\Big|_A = 0. \quad (3.21)$$

The geodesic equation at  $A'$  is given by

$$\frac{d^2x^\alpha}{d\lambda^2}\Big|_{A'} + \Gamma_{\mu\nu}^\alpha \frac{dx^\mu}{d\lambda} \frac{dx^\nu}{d\lambda}\Big|_{A'} = 0. \quad (3.22)$$

Choosing coordinates so that the coordinate  $x^0$  points along the geodesic, i.e.,  $k^\alpha = \delta_0^\alpha$ , we get

$$\frac{d^2x^\alpha}{d\lambda^2}\Big|_{A'} + \Gamma_{00}^\alpha(A') = 0. \quad (3.23)$$

Assuming the points  $A$  and  $A'$  are close, we can write

$$\Gamma_{00}^\alpha(A') \approx \frac{\partial \Gamma_{00}^\alpha}{\partial x^\beta}(A') \xi^\beta, \quad (3.24)$$

where the right-hand side is evaluated at  $A$ . Since  $\xi^\alpha = x^\alpha(A') - x^\alpha(A)$ , we have at  $A$

$$\frac{d^2\xi^\alpha}{d\lambda^2} = \frac{d^2x^\alpha}{d\lambda^2}\Big|_{A'} - \frac{d^2x^\alpha}{d\lambda^2}\Big|_A = -\frac{\partial \Gamma_{00}^\alpha}{\partial x^\beta}(A') \xi^\beta. \quad (3.25)$$

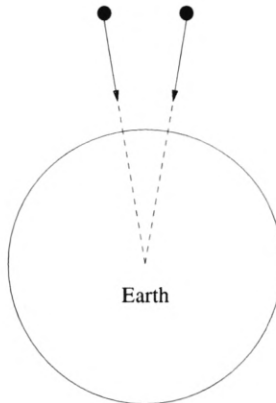


Figure 3.4: Tidal attraction of two test-particles in free fall in the earth's gravitational field.

The geodesic deviation equation (3.25) is only valid in the specific coordinate system used in the derivation. However, we would like an expression for the geodesic deviation that is valid in any frame. In the curved space of GR, one has to be careful when computing derivatives of a vector quantity like  $\xi^\alpha$  along a curve since not only the vector components may change when moving along the curve, but also the basis vectors.<sup>3</sup> Derivatives where this effect is accounted for are called *covariant derivatives* and these are valid in any coordinate system; they are frame invariant quantities. It can be shown that the frame invariant analogue of Eq. (3.25) is given by [36]

$$\Delta_k \Delta_k \xi^\alpha = -\Delta^\alpha_\beta \xi^\beta. \quad (3.26)$$

Here,  $\Delta_k$  denotes covariant derivatives along  $k$ , and  $\Delta^\alpha_\beta$  is defined by

$$\Delta^\alpha_\beta := -R^\alpha_{\mu\nu\beta} k^\mu k^\nu, \quad (3.27)$$

where  $R^\alpha_{\mu\nu\beta}$  is called the Riemann tensor which is entirely built up by the metric,  $g_{\alpha\beta}$ . The right hand side of Eq. (3.26) is called the tidal force. A simple illustration of the effect of the tidal force is given by the case of two test-particles falling freely in the gravitational field of the earth in which case the trajectories of the particles will converge, see Fig. 3.4.

<sup>3</sup>Compare with the use of spherical coordinates when parametrising three-dimensional space. In contrast to the constant basis vectors when using Cartesian coordinates, the basis vectors  $(\hat{r}, \hat{\theta}, \hat{\phi})$  will change with position.

## The Einstein equations

In Newtonian theory of gravity, the gravitational potential  $\Phi$  is related to the density  $\rho$  through

$$\nabla^2 \Phi = 4\pi\rho. \quad (3.28)$$

We want to generalise Eq. (3.28) to a set of equations for  $g_{\alpha\beta}$  given some energy and momentum distribution which can be described in tensor form through the so-called energy-momentum tensor,  $T_{\alpha\beta}$ . Comparing with Eq. (3.28), we might guess that the corresponding equations should be of the form

$$G_{\alpha\beta} = \text{const} \cdot T_{\alpha\beta}, \quad (3.29)$$

where  $G_{\alpha\beta}$  is a tensor built up by  $g_{\alpha\beta}$  and its derivatives up to second order. It can be shown that  $G_{\alpha\beta}$ , the Einstein tensor, is given by

$$G_{\alpha\beta} = R_{\alpha\beta} - \frac{1}{2}g_{\alpha\beta}R, \quad (3.30)$$

where  $R_{\alpha\beta}$  and  $R$  is called the Ricci tensor and the Ricci scalar respectively. These can be computed from the Riemann tensor. The constant can be determined from the fact that Eq. (3.28) should be recovered in the Newtonian limit of weak gravitational fields. The Einstein equations of general relativity can thus be written

$$R_{\alpha\beta} - \frac{1}{2}g_{\alpha\beta}R = 8\pi T_{\alpha\beta}. \quad (3.31)$$

The Einstein equations when applied to cosmology in a homogeneous and isotropic universe does not permit static solutions, but Einstein himself was drawn to the idea of a stable universe and introduced a term proportional to  $g_{\alpha\beta}$  to make static solutions possible. The revised Einstein equations are

$$R_{\alpha\beta} - \frac{1}{2}g_{\alpha\beta}R - \Lambda g_{\alpha\beta} = 8\pi T_{\alpha\beta}, \quad (3.32)$$

where  $\Lambda$  is known as the *cosmological constant*. After the discovery of the expansion of the universe, the interest in  $\Lambda$  declined, but after recent indications that the expansion might be accelerating, it has received a lot of interest as a potentially very important contributor to the dynamical history of the universe. In the following, we will incorporate  $\Lambda$  into  $T_{\alpha\beta}$  by defining

$$\rho_\Lambda := \frac{\Lambda}{8\pi}. \quad (3.33)$$

Since  $\Lambda$  effectively is a parameter describing the energy density of the vacuum,  $\rho_\Lambda$  is often referred to as the *vacuum energy density*.

### 3.3 Cosmological models

Before attempting to solve Eq. (3.32), we would like to constrain the metrics to put into the equations. Our starting-point is the *cosmological principle*; the hypothesis that the universe is spatially homogeneous and isotropic. That is, the universe looks the same way at every point and in every direction. It can be shown that in such a universe, parametrised by coordinates  $t, r, \theta$  and  $\phi$ , the line element is given by the so-called *Robertson-Walker (RW) metric*,

$$ds^2 = -dt^2 + a^2(t) \left[ \frac{dr^2}{1 - kr^2} + r^2 d\theta^2 + r^2 \sin^2 \theta d\phi^2 \right]. \quad (3.34)$$

$a(t)$  is a dimensionless scale factor depending on the time  $t$ , and  $k$  is related to the spatial curvature with  $k = -1, +1, 0$  depending on whether space is negatively curved, positively curved or flat, respectively. For  $k = +1$ , the universe will be closed in the sense that it has finite volume. If  $k = 0$  or  $-1$ , the universe will be open, i.e., its volume is infinite. In order to solve the Einstein equations for the unknown scale factor  $a(t)$  in the metric we need also to assume an explicit form for the  $T_{\alpha\beta}$ . Note however that the energy-momentum tensor itself in general depends on the metric  $g_{\alpha\beta}$ . It is therefore not possible to first specify  $T_{\alpha\beta}$  and then solve for the gravitational field. One has to solve for  $T_{\alpha\beta}$  and  $g_{\alpha\beta}$  simultaneously, making the problem much more difficult.

#### The energy-momentum tensor

In the standard model of our universe, the energy-momentum content is described as a perfect fluid, i.e., a fluid with no viscous forces, where galaxies and clusters of galaxies can be considered as fluid particles. In analogy with the four-momentum of a particle, we describe a perfect fluid with an energy-momentum tensor  $T^{\alpha\beta}$  of the form

$$T^{\alpha\beta} = \begin{pmatrix} T^{00} & T^{0j} \\ T^{i0} & T^{ij} \end{pmatrix} = \begin{pmatrix} \text{energy density} & \text{energy current} \\ \text{momentum density} & \text{momentum current} \end{pmatrix}. \quad (3.35)$$

It can be shown (see, e.g., [5]) that we can write  $T^{\alpha\beta}$  as

$$T^{\alpha\beta} = \rho u^\alpha u^\beta - p(u^\alpha u^\beta + g^{\alpha\beta}), \quad (3.36)$$

where  $\rho$  is the proper density,  $p$  is the pressure and  $u^\alpha$  is the four-velocity of the fluid particles. A number of perfect fluids can be represented by the sum

$$T^{\alpha\beta} = \sum_i \rho_i u^\alpha u^\beta - p_i(u^\alpha u^\beta + g^{\alpha\beta}). \quad (3.37)$$

Assuming a homogeneous and isotropic universe,  $\rho$  and  $p$  will be functions of  $t$  only. For the perfect fluids of relevance to cosmology, we can assume a so-called *equation of state* relating the density and the pressure;

$$p_i = \alpha_i \rho_i. \quad (3.38)$$

The most important cases are:

- Pressure-less matter:  $p = 0$
- Radiation:  $p = \rho/3$
- Cosmological constant:  $p = -\rho$

When discussing a dark energy component,  $\rho_X$ , one often allows for the equation of state parameter,  $\alpha_X$ , to vary with redshift

$$p_X = \alpha_X(z) \rho_X. \quad (3.39)$$

We are now in a position to derive the standard model of cosmology, the *Friedmann-Lemaître (FL) model*.

## The Standard Model

When inserting Eq. (3.36) with a line-element of the form Eq. (3.34) into the Einstein equations (3.32), we obtain two differential equations for the scale factor  $a(t)$ ; the *Friedmann equation*,

$$3 \left( \frac{\dot{a}}{a} \right)^2 = 8\pi \sum_i \rho_i - \frac{3k}{a^2}, \quad (3.40)$$

and the *Raychaudhuri equation*

$$3 \frac{\ddot{a}}{a} = -4\pi \sum_i (\rho_i + 3p_i). \quad (3.41)$$

The quantity  $\dot{a}(t)/a(t)$  is a measure of the expansion rate of the universe and is called the *Hubble parameter*,

$$H(t) := \frac{\dot{a}(t)}{a(t)}. \quad (3.42)$$

The Hubble parameter at the present time  $t_0$  is, somewhat erroneously, called the *Hubble constant*,  $H_0 := H(t_0)$ . Defining a critical density  $\rho_{\text{crit}}$  of the universe,

$$\rho_{\text{crit}} := \frac{3H^2}{8\pi}, \quad (3.43)$$

the Friedmann equation (3.40) can be written

$$\frac{k}{H^2 a^2} = \Omega - 1, \quad (3.44)$$

where  $\Omega$  is the total energy density in units of the critical density,

$$\Omega := \sum_i \frac{\rho_i}{\rho_{\text{crit}}}. \quad (3.45)$$

Hence, the sign of  $k$ , and therefore the overall geometry of the universe is determined by the value of  $\Omega$ . Sometimes, one incorporates the curvature into  $\Omega$  by defining a curvature density

$$\rho_k = -\frac{3k}{8\pi a^2}. \quad (3.46)$$

In the following, we will make extensive use of the so-called *redshift parameter*  $z$ , defined by

$$1 + z := \frac{\lambda_{\text{obs}}}{\lambda_{\text{emit}}}, \quad (3.47)$$

where  $\lambda_{\text{emit}}$  and  $\lambda_{\text{obs}}$  denotes wavelengths of light (from, e.g., a SN) at emission and observation, respectively. Using the FL model, one can derive a relation between the redshift and the scale factor:

$$1 + z = \frac{a(t_{\text{obs}})}{a(t_{\text{emit}})}. \quad (3.48)$$

Equation (3.48) tells us that in a FL universe, the wavelength of light travelling cosmological distances, is expanded by the same factor as the universe during the time elapsed from emission to observation.

Using the RW line-element (3.34), one can derive an energy conservation equation of the following form (see, e.g., [5])

$$\frac{d}{dt}(\rho_i a^3) = -p_i \frac{d}{dt}a^3. \quad (3.49)$$

That is, the rate of change of energy in the volume  $V = a^3$  is equal to minus the pressure times the change of volume, for each component of the fluid. Using the equation of state (3.38), we can write the energy conservation equation (3.49) as

$$\rho_i \propto a^{-3(1+\alpha_i)}. \quad (3.50)$$

From the Friedmann equation (3.40) and the relation between redshift and the scale factor in a FL universe (3.48), the expansion rate of the universe at any epoch can be related to the expansion rate today by

$$H(z) = H_0 \sqrt{\sum_i \Omega_i (1+z)^{3(1+\alpha_i)}} =: H_0 \sqrt{g(z)}, \quad (3.51)$$

which also defines the quantity  $g(z)$ . Using Eq. (3.48), we can also derive the following relation,

$$H = \frac{-1}{(1+z)} \frac{dz}{dt}, \quad (3.52)$$

or, equivalently

$$\frac{dt}{dz} = \frac{-1}{H_0(1+z)\sqrt{g(z)}}. \quad (3.53)$$

Armed with expressions describing the expansion history of the universe and the relation between time and redshift, we are now able to derive distance-redshift relations in an expanding universe.

## 3.4 Distance relations

Cosmological distances are, in contrast to, e.g., angular separations, luminosities or redshifts, not directly observable. However, there are several different indirect ways to measure cosmological distances. The *angular diameter distance*,  $d_A$ , uses the fact that the angular size of an object decreases with increasing distance,

$$d_A(z) := \frac{D}{\delta\theta}, \quad (3.54)$$

where  $D$  is the size of the object and  $\delta\theta$  is the angle it subtends on the sky. The *luminosity distance*,  $d_L$ , is based on the effect that objects appear weaker the further away they are. A source with intrinsic luminosity  $L$  is observed to have flux  $S$ ,

$$S = \frac{L}{4\pi d_L^2(z)}, \quad (3.55)$$

where  $d_L(z)$  defines the luminosity distance for redshift  $z$ . It is related to the angular diameter distance by  $d_L = d_A(1+z)^2$ .

Using a specific metric, it is possible to obtain a relation for the luminosity distance (and consequently also the the angular diameter distance) as a function of redshift  $z$ . The use of the RW metric (3.34) yields the so-called *standard distance* relation. It is characterised by the same parameters as the cosmological model it is built upon; the Hubble constant which sets the overall normalisation of the distance scale and the energy densities which govern the redshift dependence. The luminosity distance to an event at redshift  $z$  is given by [5]

$$d_L = a_0(1+z) f \left( \frac{1}{a_0} \int_0^z \frac{dz'}{H(z')} \right), \quad (3.56)$$

$$f(x) = \begin{cases} \sin(x), & k = 1, \\ x, & k = 0, \\ \sinh(x), & k = -1. \end{cases} \quad (3.57)$$

In some sense, the use of the RW metric is very crude, since the universe is far from homogeneous, at last on smaller scales. One concern is whether the overall expansion rate of the universe might be influenced by the inhomogeneities, i.e., if the solution for the overall dynamical behaviour of the universe is erroneous due to the fact that we average the energy-momentum tensor before putting it into the Einstein equations. This question is far from settled and interested readers are referred to [6] and references therein.

Another concern is related to the fact that light propagating through inhomogeneous spacetime feels the local metric rather than the averaged, smooth RW metric. One therefore tries to set up a relation for the luminosity or angular diameter distance that will hold, at least approximately, in inhomogeneous universes which are homogeneous on large scales. Following Dyer and Roeder [11], we assume that a certain mass-fraction  $\alpha$  of all matter is distributed uniformly, whereas the remaining fraction  $1-\alpha$  is

bound in clumps where the scale of the clumpiness is set by the observed angular size of the source. For example, a halo of compact, solar-mass MACHOs (see Sec. 3.5) in an intervening galaxy would be counted among the homogeneously distributed matter if one would be concerned with the distance to background galaxies, but would be regarded as clumped when considering distances to a population of very compact background sources, e.g., Type Ia SNe (see Sec. 5 in **Paper I**).

Making the simplifying assumption that light travels far away from all clumps, one can obtain a differential equation for the Dyer-Roeder (DR) distance-redshift relation,  $\tilde{d}_L(z)$ , containing the additional smoothness parameter  $\alpha$ . An increase in clumpiness  $1 - \alpha$  for fixed overall energy densities, leads to an increase of  $\tilde{d}_L(z)$ . Note that the DR distance basically is the distance one would obtain in a universe where light-rays travelling through space only feels a fraction  $\alpha$  of the matter, but where the overall expansion of the universe is governed by the total matter density. Note also that setting  $\alpha = 1$ , one obtains the standard distance or *filled-beam* approximation. Setting  $\alpha = 0$ , i.e., all matter bound in clumps, one obtains the *empty-beam* approximation.

In **Paper V**, we determine the best-fit value of the homogeneity parameter  $\alpha$  in the DR distance-redshift relation for different redshifts, inhomogeneity models and cosmological parameter values. Using the simulation package SNOC (Sec. 4.3), we have obtained angular-diameter distances with different inhomogeneity models and different values of the cosmological parameters. In inhomogeneous models, there will not be a one-to-one correlation between the distance and the redshift since gravitational lensing will cause a dispersion in the angular sizes. Figure 3.5 shows one simulated data set of angular-diameter distances together with the DR angular-diameter distance for three different values of  $\alpha$ . Using  $\chi^2$ -tests, we determine the best-fit  $\alpha$ -value for each of our simulated data sets. Note that in the corresponding Fig. 2 in **Paper V**, the value of  $1 - \alpha$  for the upper and the lower line have been interchanged.

The relation between  $\alpha$  and the fraction of compact objects,  $f_p$ , is found to be approximately linear, parametrised with reasonable accuracy by  $1 - \alpha = a \cdot f_p$ , where  $a \approx 0.6$ .

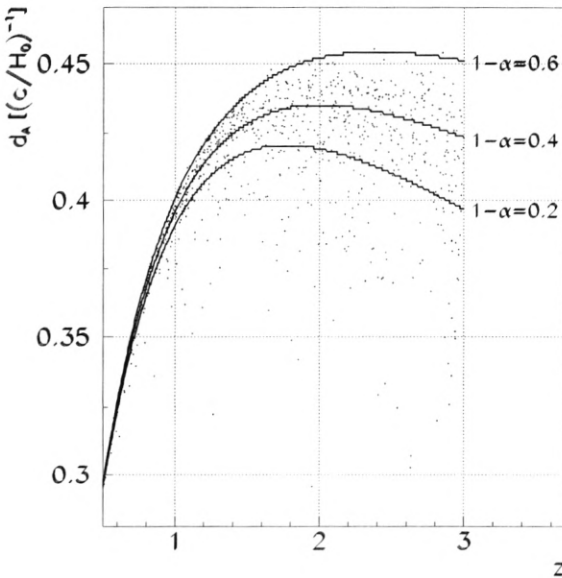


Figure 3.5: The dispersion in  $d_A$  for  $(\Omega_M, \Omega_\Lambda) = (0.3, 0.7)$  with a fraction 0.6 of the matter density in galactic DM halos and a fraction 0.4 in compact objects.

### 3.5 Dark matter

The universe was both denser and smoother in the past than it is today. However, there were small fluctuations in the energy density of both radiation and matter. Under the action of gravity, regions which were slightly overdense accreted matter from their surroundings and the small fluctuations in the matter density grew. Thus, overdense regions grew more overdense and underdense regions grew more underdense. This constant amplification of the initially very small fluctuations gave rise to the structures we see in the universe today. The initial fluctuations is often believed to be seeded by a mechanism called *inflation*. This is a period of exponential growth of the scale factor in the early universe which amplified quantum vacuum fluctuations into the seeds for large scale structure.

The way structures grow depends on the amount and type of matter

present. When all of these ingredients are specified, one can use N-body simulations or analytic approximations to compute the full evolution of large scale structure as well as structure on smaller scales, e.g., galaxy halos. The amplitude of the fluctuations at the time of decoupling have been inferred by measuring the temperature fluctuations of the CMBR. The fluctuations seem to be too small to allow for the observed structures to form if made up of only baryons and radiation indicating the need for some weakly interacting DM particle. The only candidate of the known particles in the standard model of particle physics, the neutrino, is disfavoured because of its low mass which inhibits structure formation. Thus, the major part of the matter in the universe is probably in the form of some undetected elementary particles. In this respect, DM provides a fundamental link between cosmology and particle physics where there is also theoretical motivations for new elementary particles.

We use the term WIMPs, to describe hypothetical weakly interacting massive particles that could make up the DM. Examples of WIMPs are axions and supersymmetric neutralinos. In contrast to WIMP candidates that can often be considered as relatively smooth on sub-halo scales, there is also the possibility that some DM clump on small scales. These are generically termed MACHOs or massive astrophysical compact halo objects and can, e.g., be brown dwarfs, low mass stars or black holes.

In **Paper III** it is investigated how one can use gravitational lensing of Type Ia SNe to discern between these possibilities or even determine the amount of DM that is in the form of compact objects.

When studying galactic dynamics, we are justified in using Newtonian gravity since the gravitational fields generally are weak and the velocities low. We can thus relate the rotational velocity,  $v(r)$ , of the stars and gas in the disks of spiral galaxies to the mass,  $M(r)$ , within radius  $r$  by

$$v(r) = \sqrt{\frac{M(r)}{r}}. \quad (3.58)$$

Observationally, the rotation velocity is nearly constant out to radii extending far beyond the star-light, indicating that  $M(r)$  increases linearly with  $r$  whereas the integrated luminosity is constant. In order to explain these flat rotation curves, we need large amounts of matter that is dark in the respect that we only see its gravitational effects.<sup>4</sup> When studying

---

<sup>4</sup>An alternative approach uses modifications of gravitational dynamics on galaxy scales, see, e.g., [22].

ellipticals galaxies, it is not possible to use rotation curves as dynamical indicators. Instead one uses temperature distributions of hot x-ray emitting gas and weak gravitational lensing of background galaxies [20, 33]. Observations indicate that also elliptical galaxies contain large amounts of DM.

We can quantify the amount of DM in a system through its mass-to-light ratio given in units of  $M_\odot/L_\odot$ , the mass-to-light ratio of the sun. A typical stellar population have a mass-to-light ratio of a few  $M_\odot/L_\odot$ , galaxies may have ratios up to  $\sim 100 M_\odot/L_\odot$  and for galaxy clusters, the mass-to-light ratio is typically a few hundred  $M_\odot/L_\odot$ .

In order to estimate the density contribution from a particular type of system, we multiply the measured luminosity density for the system with its mass-to-light ratio. For typical stellar populations one finds  $\Omega_* h = 0.002 - 0.006$ , where  $h$  is the Hubble constant in units of  $100 \text{ km s}^{-1} \text{Mpc}^{-1}$ .

This is to be compared with the total density of baryons which is constrained by big bang nucleosynthesis to be  $\Omega_b h^2 = 0.019 \pm 0.0024$  [7] and from CMBR measurements  $\Omega_b h^2 = 0.02^{+0.06}_{-0.01}$  [39]. This indicates that most of the baryonic matter is dark.

Assuming that the mass-to-light ratio of galaxy clusters ( $M/L \simeq 300 M_\odot/L_\odot$ ) is representative of the universe as a whole we get  $\Omega_M = 0.1 - 0.4$ . This value is in agreement with constraints on the matter density  $\Omega_M$  from cluster abundances [4] and large scale structure [25].

As for today, one of the outstanding questions in cosmology is: What is the DM? As we will learn in the next chapter, another outstanding question remains to be answered, namely: What makes the universe accelerate?

# Chapter 4

## Determination of cosmological parameters

In this chapter we discuss cosmological parameter determination with special emphasis on Type Ia supernova observations.

### 4.1 Introduction

One of the major goals of cosmology is to determine the values of the cosmological parameters of our universe, such as the energy densities (e.g.,  $\Omega_M$  and  $\Omega_\Lambda$ ) and the Hubble constant  $H_0$ . First we estimate which energy components we expect to dominate the total energy density of the universe at different epochs by studying Eq. (3.50). For pressure-less matter,  $\alpha = 0$  and

$$\rho_M \propto \frac{1}{a^3}. \quad (4.1)$$

For radiation energy,  $\alpha = 1/3$  and

$$\rho_{\text{rad}} \propto \frac{1}{a^4}. \quad (4.2)$$

In the early universe (the first couple of hundred thousand years), radiation was the dominating form of energy. However, the contribution from radiation to the total energy density in the universe today is negligible. Since for a vacuum energy component

$$\rho_\Lambda = \text{constant}, \quad (4.3)$$

if it exists, it will sooner or later be the dominant energy component.

Until recently, one has only been able to give large error estimates of the cosmological parameters, but recent observations of the CMBR and the magnitude-redshift relation for Type Ia SNe have set a new standard for the determination of the energy densities of our universe. Measurements of the CMBR show that the universe is very close to flat, i.e.,  $\Omega \simeq 1$  [23, 37, 28]. This is consistent with the results from SN measurements, which also indicate that the major part of the energy density is in the form of a cosmological constant, or some other dark energy component with negative pressure [26, 30].

There are also theoretical arguments for why the average energy density in the early universe should be equal to or very close to the critical density defined in Eq. (3.43). To understand this, we note that a possible curvature density component will evolve with redshift as [see Eq. (3.46)],  $\rho_k \propto (1+z)^2$ , whereas the density of pressure-less matter will evolve as  $\rho_M \propto (1+z)^3$  and the radiation density as  $\rho_{\text{rad}} \propto (1+z)^4$ . During periods of matter domination we can write Eq. (3.44) as

$$\Omega - 1 = \frac{k}{H^2 a^2} \simeq \frac{k/a^2}{8\pi\rho_{\text{rad}}/3} \propto a \propto (1+z)^{-1}, \quad (4.4)$$

whereas in the early universe when, though negligible today, the energy density of the early universe was completely dominated by radiation,  $\Omega - 1 \propto a^2 \propto (1+z)^{-2}$ . It is safe to assume that  $\Omega$  today has a value between 0 to 10 and thus the value of  $\Omega$  in the early universe will be very close to one, e.g., at the time of photon decoupling we will have  $\Omega \simeq 1 \pm 10^{-3}$  and at nucleosynthesis  $\Omega \simeq 1 \pm 10^{-16}$ . This tells us that in order to get a value of  $\Omega$  that is close to, but not exactly, one today, we need a value of  $\Omega$  in the early universe that is extremely fine-tuned to a value very close to one. If however,  $\Omega$  would be exactly one, it would stay at this value through the entire dynamical history of the universe. A mechanism that could cause  $\Omega$  to be sufficiently close to one in order to stay that way is inflation. Since we know from large scale structure that  $\Omega_M \sim 0.3$ , it is believed that  $\sim 70\%$  of the energy density is in some dark energy component.

Cosmology today is in a state where we know very little about the most prominent energy constituents. As the error bars in cosmological parameter estimation are shrinking, the importance of a proper understanding of possible sources of systematic errors is growing. Before we

investigate this effect, we discuss how Type Ia SNe are used to determine the cosmological parameters of our universe.

## 4.2 Cosmological parameters from Type Ia supernovae

SNe come in two main varieties. Those whose optical spectra exhibit hydrogen are classified as Type II, while hydrogen deficient SNe are designated Type I. Type I SNe are further subdivided according to the appearance of the early-time spectrum. Type Ia are characterised by strong absorption near 6150 Å, attributed to Si II. Type Ib lack this feature but instead show prominent He I lines, and Type Ic have neither the Si II nor the He I lines. Type II are believed to be the result of core collapse in massive supergiant stars. The latter mechanism probably produces most Type Ib/c SNe as well, but the progenitor stars previously lost their outer layers of hydrogen.

Type Ia are believed to occur in binary systems where a white dwarf accretes matter from the binary companion until critical conditions are reached and the progenitor star contracts, ignites and finally explodes. The fact that Type Ia SNe are a quite homogeneous class of events, indicates that the most important critical condition is for the progenitor star to reach the Chandrasekhar mass limit.

It has long been recognised that Type Ia SNe may be very useful distance indicators for a number of reasons:

- First, they have a relatively small dispersion among their peak absolute magnitudes ( $\sigma_m \simeq 0.15$ ).
- Second, they are very luminous, allowing detection at very large distances.
- Third, the distinct spectral lines allow for accurate redshift determinations.
- Fourth, they exist at large distances, up to  $z \simeq 1.7$  (see **Paper IV**).

There are two major teams involved in the systematic investigation of high redshift Type Ia SNe for the determination of cosmological parameters [26, 30]. Results from both groups indicate a non-zero cosmological constant since SNe are observed to be dimmer than expected in an empty

universe, the explanation being that a dark energy density with negative equation of state accelerates the expansion.

## The magnitude-redshift relation

Since the luminosity distance is cosmology dependent, by measuring the luminosities and redshifts of so-called standard candles, i.e., objects of known intrinsic strength, one can discern between different cosmologies [14].

Astronomers measure luminosities in logarithmic units, *magnitudes*. The apparent magnitude,  $m$ , is a measure of the observed luminosity and the absolute magnitude,  $M$ , is the apparent magnitude if observed from a distance of 10 pc.<sup>1</sup> The apparent and absolute magnitudes are related by

$$\begin{aligned} m(z) &= M + 5 \log_{10} [d_L(z, H_0, \Omega_i)] + 25 \\ &=: M + 5 \log_{10} [\mathcal{D}_L(z, \Omega_i)] - 5 \log_{10} H_0 + 25, \end{aligned} \quad (4.5)$$

where the luminosity distance  $d_L$  is measured in Mpc.  $\mathcal{D}_L := H_0 d_L$  is the part of the luminosity distance that remains after multiplying out the dependence on the Hubble constant (expressed here in units of  $\text{km s}^{-1} \text{Mpc}^{-1}$ ). In the low redshift limit, Eq. (4.5) reduces to a linear Hubble relation between  $m$  and  $\log_{10} z$ :

$$\begin{aligned} m(z) &= M + 5 \log_{10} z - 5 \log_{10} H_0 + 25 \\ &=: \mathcal{M} + 5 \log_{10} z, \end{aligned} \quad (4.6)$$

where we have expressed the intercept of the Hubble line as the magnitude “zero point”,  $\mathcal{M} := M - 5 \log_{10} H_0 + 25$ . This quantity can be measured from the apparent magnitude of low redshift standard candles, without knowing the value of  $H_0$ . Thus, with a set of apparent magnitude and redshift measurements  $m(z)$  for high-redshift candles, and a similar set of low-redshift measurements to determine  $\mathcal{M}$ , we can find the best fit values of  $\Omega_i$  to solve the equation

$$m(z) - \mathcal{M} = 5 \log_{10} [\mathcal{D}_L(z, \Omega_i)]. \quad (4.7)$$

Figure 4.1 shows the Hubble diagram for 42 high redshift SNe observed by the *Supernova Cosmology Group* and 12 low redshift SNe from the

---

<sup>1</sup>Astronomers measure distances in parsec (pc). One pc is  $\sim 3.26$  light-years.

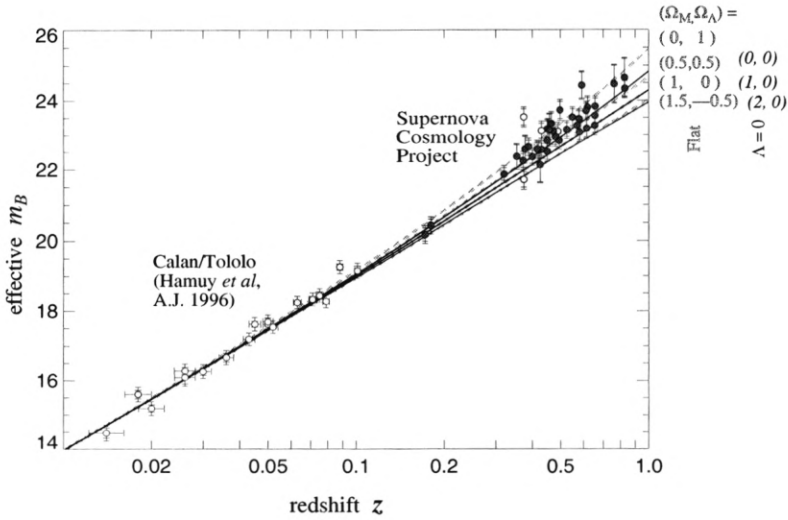


Figure 4.1: Hubble diagram for 42 high redshift SNe observed by the *Supernova Cosmology Group* [26].

Calán/Tololo Supernova Survey [26]. In the diagram, the theoretical predictions for different values of  $\Omega_M$  and  $\Omega_\Lambda$  are plotted together with the observed data. It can be seen that SNe are fainter than expected in a universe with no cosmological constant.

The corresponding confidence region in the  $(\Omega_M, \Omega_\Lambda)$ -plane is shown in Fig. 4.2 where we can see that the case of a vanishing cosmological constant is ruled out at high confidence level. Similar results from Type Ia SN observations have been obtained by an independent analysis [30].

## SNAP

Even though the results from the current SN data are quite impressive, one would need better statistics in order to improve the significance of the results. Also, it is very important to be able to control any possible systematic effects.

The Supernova/Acceleration Probe (SNAP) is a proposed satellite

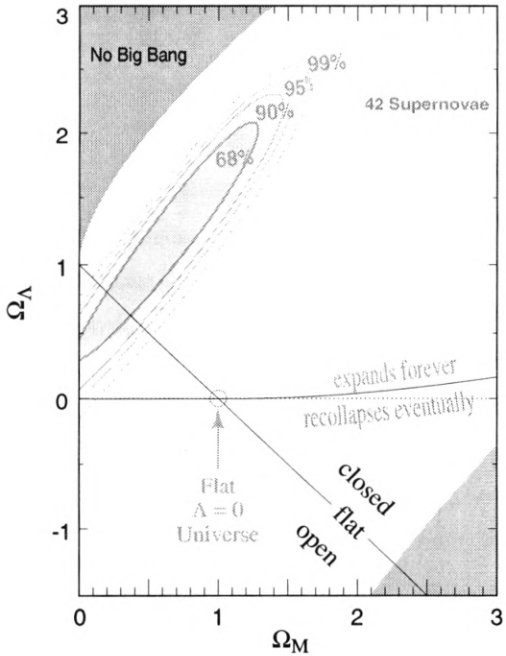


Figure 4.2: Confidence region in the  $(\Omega_M, \Omega_\Lambda)$ -plane corresponding to the SNe data plotted in Fig. 4.1.

telescope with a one square degree field-of-view with 1 billion pixels. SNAP would be capable of discovering, following the light curves and obtaining spectra for the order of 2000 SNe per year in the redshift range  $0.1 < z < 1.7$  [27]. This data can be used to gain further knowledge of, e.g., the matter density  $\Omega_M$  and the curvature of the Universe  $\Omega_k$ , but also to give insight into the nature of the negative pressure energy component by constraining the equation of state [13]. Also, the increased statistics (two orders of magnitude) and added control of systematic effects can help to eliminate possible alternative explanations. An example of this can be found in **Paper VI** where it is shown how to test for intergalactic dust obscuration affecting the measurement of high- $z$  SNe down to  $\Delta m \sim 0.02$ , the target for systematic uncertainties for SNAP.

## 4.3 Systematic effects

The effect of a cosmological constant, or any other dark energy component with negative pressure, is to push SNe at a given redshift toward higher magnitudes in the Hubble diagram, i.e., to make SNe look fainter. Since there are alternative explanations to why SNe may appear dimmer, it is important to control these effects when determining the cosmological parameters. These includes the effects on light travelling cosmological distances studied in this thesis, namely gravitational lensing, extinction by dust and the conversion of photons to a hypothetical light axion.

Of course, *any* effect capable of altering the apparent magnitude of sources at cosmological distances need to be understood to control the bias in the Hubble diagram, including the possibility of luminosity evolution of Type Ia SNe.<sup>2</sup>

### SNOC

SNOC is a package for simulation of SN data, capable of, e.g., estimating potential systematic effects for cosmological parameter determination from Type Ia SN observations. A detailed description of the code can be found in **Paper VIII** where all the input and output parameters are explained and the methods used in calculating different quantities are discussed. Here, we will briefly outline the most important aspects of the code.

The programme works in a Monte-Carlo fashion, i.e., using a random number generator, a sample of synthetic observational events can be produced in order to obtain the probability distribution of certain effects. One event corresponds to one SN characterised by its redshift and type (e.g., Type Ia ,Type Ibc). The luminosity distance to the redshift is calculated from the user supplied set of cosmological parameters assuming a standard FL universe with arbitrary choice of dark energy. The SN apparent magnitudes through a standard, or user specified, broad-band filter is calculated using cross-filter K-corrections. Effects from gravitational lensing, dust extinction and photon-axion oscillations are calculated by tracing light-rays from the host galaxy of the SN to the observer at earth.

The light-ray path is divided into cells corresponding approximately to average distances between galaxies. Each cell is characterised by its

---

<sup>2</sup>The evolutionary effects include the fact that progenitor stars on average may have lower metallicities when going to higher redshifts.

- mass density profile, the source of gravitational lensing (Ch. 5),
- dust density and differential extinction coefficient, treated separately for the actual galaxy and the region around it (Ch. 6),
- average magnetic field and electron density, relevant in scenarios such as the photon-axion oscillation mechanism (Ch. 7).

The SNOC package also includes a software tool for cosmology fitting, based on the output from the Monte-Carlo code. Two different types of maximum-likelihood analyses can be done using different measurement variables:

1. Type Ia SNe as standard candles can be used to fit, e.g., the cosmological parameters  $\Omega_M$ ,  $\Omega_X$ ,  $\alpha_X$ , by using real or simulated events.
2. Multiple lensed SNe can be used to fit  $H_0$ ,  $\Omega_M$ ,  $\Omega_X$  and  $\alpha_X$  (=constant).

In the section on **Paper IX**, it is described how to take into account the fact that the data could be subject to systematic effects from gravitational lensing when fitting cosmological parameters with Type Ia SNe as standard candles.

In the following chapters we will discuss the systematic effects from gravitational lensing, dust extinction and photon-axion oscillations in some more detail.

# Chapter 5

## Gravitational lensing

The theory of gravitational lensing is summarised and its effects on Type Ia supernova measurements are investigated.

### 5.1 Introduction

In this chapter, we will investigate the effects from gravitational lensing on Type Ia SN measurements. Since the determination of cosmological parameters from the CMBR involves relatively large angle measurements, the effects from gravitational lensing will be small. This is due to the fact that the universe on large angular scales can be considered as homogeneous to very good approximation (cf. the derivation of the DR distance relation). However, since Type Ia SNe are very compact sources, the universe cannot be considered as homogeneous on the angular scales involved in the measurements, and gravitational lensing effects might potentially be of importance.

### 5.2 History of gravitational lensing<sup>1</sup>

It has been long known that not only optical lenses are able to deflect light but that gravity could have the same effect. In the first edition of *Opticks*, Newton wrote in his first *Query*:

---

<sup>1</sup>A comprehensive collection of references covering the material in this section can be found in [35].

Do not Bodies act upon Light at a distance, and by their action bend its rays; and is not this action (*caeteris paribus*) strongest at the least distance?

The deflection of light by a spherical body of mass  $M$  can be calculated employing Newtonian gravity and assuming that light consists of material particles, see Appendix A. The result

$$\alpha \approx \frac{2M}{\xi}, \quad (5.1)$$

where  $\xi$  is the impact distance (approximately equal to the shortest distance from the center of the mass to the light path) applied to the case of a light-ray grazing the surface of the sun predicts a deflection of  $\simeq 0.87$  arcseconds.

Later Einstein applied the full field equations of general relativity and discovered that the deflection angle is twice the previous results.<sup>2</sup> This result was confirmed in 1919 when the apparent angular shift of stars close to the limb of the sun was measured during a total solar eclipse. The quantitative agreement between the measured shift and Einstein's prediction was perceived as strong evidence in support of the general theory of relativity.

It would be another 60 years before Walsh, Carswell and Weymann in 1979 announced the detection of the first cosmological gravitational lens candidate, the quasar QSO 0957+561. The source has two optical counterparts, separated by 6 arcseconds. Evidence for the lensing nature of this system is provided by (i) the similarity of the spectra of the two images , (ii) the equal ratio of optical and radio fluxes and (iii) the subsequent detection of a lensing galaxy.

Today, a large number of gravitational lens systems have been observed, including multiple images of quasars, background galaxies stretched into elongated arcs and stars being magnified by compact objects.

### 5.3 Theory of gravitational lensing

We have seen how light-rays can be characterised as solutions to the geodesic equation (3.19). Here we will take a different approach, of particular interest because of the close analogy with optical lensing.

---

<sup>2</sup>In 1911, Einstein had derived the same value as in Newtonian gravity using the principle of equivalence but assuming a Euclidean metric [12].

### The deflection angle

The deflection angle caused by an optical lens is determined by:

- The form of the lens
- The material of the lens
- The wavelength of the deflected light

The latter two properties can be summarised into a wavelength dependent *index of refraction*, usually denoted  $n(\lambda)$ . Since gravitational lensing is an effect of spacetime curvature only, the deflection angle caused by a gravitational lens is independent of the type of matter constituting the lens and also of the wavelength of the deflected light. Thus, the deflection angle of a gravitational lens is determined by:

- The distribution of mass within the lens

The effects of spacetime curvature on a light-ray can be described in terms of an effective index of refraction which can be derived by considering a FL universe where the effects from inhomogeneities are represented by perturbations of the metric. This approach is valid if

- the Newtonian potential  $\Phi$  is small, i.e.,  $|\Phi| \ll 1$ , and
- the peculiar velocity  $v$  of the inhomogeneities are small,  $v \ll 1$ ,

which are conditions satisfied in most cases of astrophysical interest. Modelling the matter distribution as a perfect fluid of the form of Eq. (3.36) and solving the Einstein equations (3.32) with the assumptions stated above, we obtain the so-called post-Minkowskian metric [35]

$$ds^2 \approx -(1 + 2\Phi)dt^2 + (1 - 2\Phi) \left[ \frac{dr^2}{1 - kr^2} + r^2 d\theta^2 + r^2 \sin^2 \theta d\phi^2 \right]. \quad (5.2)$$

Since  $ds^2 = 0$ , the effective speed of a light-ray in a gravitational field is to first order given by

$$v = \frac{1}{n} \simeq 1 + 2\Phi, \quad (5.3)$$

and thus,

$$n = 1 - 2\Phi = 1 + |2\Phi|. \quad (5.4)$$

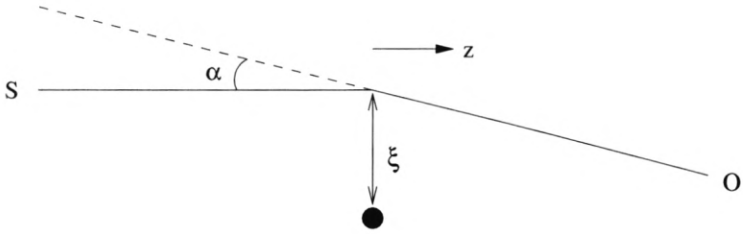


Figure 5.1: Light deflection by a point-mass.

In analogy with optical lenses, the deflection angle,  $\vec{\alpha}$ , is given by the integral of the gradient of  $n$  perpendicular to the direction of propagation,

$$\vec{\alpha} = \int \nabla_{\perp} n dl = 2 \int \nabla_{\perp} \Phi dl. \quad (5.5)$$

In most cases, the deflection angle is very small. We are therefore justified in simplifying the computation of the deflection angle by integrating not along the deflected ray, but along an unperturbed ray with the same impact parameter. As an example, we compute the deflection angle of a point-mass  $M$ , see Fig. 5.1. The Newtonian potential of the lens is given by

$$\Phi(\xi, z) = -\frac{M}{\sqrt{\xi^2 + z^2}}, \quad (5.6)$$

where  $\xi$  is the impact parameter and  $z$  indicates distance along the unperturbed light-ray from the point of closest approach. The gradient of  $\Phi$  perpendicular to the unperturbed ray is given by

$$\nabla_{\perp} \Phi(\xi, z) = \frac{M \vec{\xi}}{(\xi^2 + z^2)^{3/2}}, \quad (5.7)$$

where  $\vec{\xi}$  is orthogonal to the direction of propagation and points toward the point-mass. Inserting Eq. (5.7) into Eq. (5.5), we get

$$\vec{\alpha} = M \vec{\xi} \int \frac{dz}{(\xi^2 + z^2)^{3/2}} = 4M \frac{\vec{\xi}}{\xi^2}. \quad (5.8)$$

In fact, this is valid for any circularly symmetric mass distribution if we let  $M$  denote the projected mass inside radius  $r = |\xi|$ . Introducing the Schwarzschild radius

$$R_S = 2M, \quad (5.9)$$

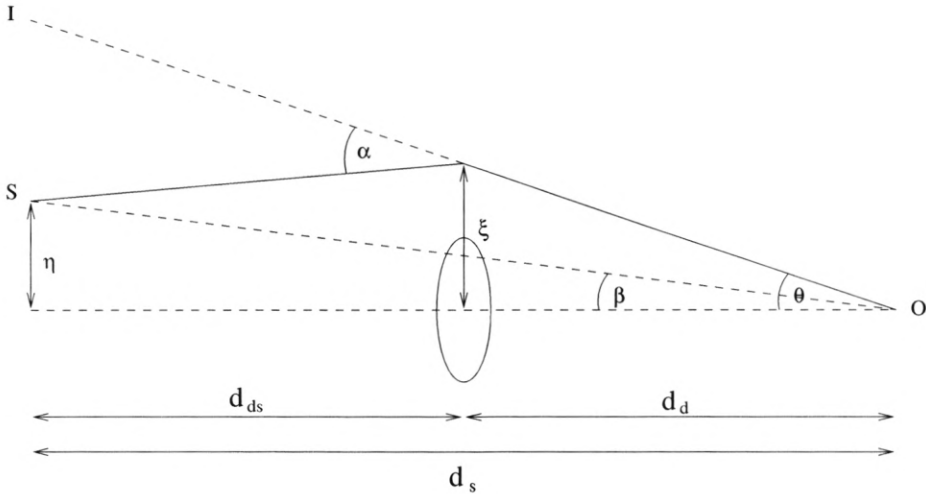


Figure 5.2: Geometry of a gravitational lens system.

and noting that the Schwarzschild radius of the sun is approximately 3 km, we can write the magnitude of the deflection angle from a point-mass as

$$\alpha = 2 \frac{R_S}{\xi} \approx 3 \frac{M}{M_\odot} \frac{\text{km}}{\xi}. \quad (5.10)$$

We see that deflection angles generally are very small, e.g., light-rays grazing the surface of the sun are deflected by  $\simeq 1.74$  arcseconds.

### The lens equation

The geometry of a typical gravitational lens system is shown in Fig. 5.2. A light-ray from a source  $S$  at redshift  $z_s$  is incident on a deflector at redshift  $z_d$  with impact parameter  $\vec{\xi}$ . It is deflected by an angle  $\vec{\alpha}$  at the lens and reaches the observer at  $O$ , who sees the image of the source at the apparent position  $\vec{\theta}$  on the sky. The true position of the source, i.e., its position on the sky in absence of the lens, is denoted  $\vec{\beta}$ . We assume that the influence of the lens can be satisfactorily described by the deflection angle  $\vec{\alpha}$  and that the light-ray can be approximated by its asymptotic directions at the source and the observer. The angular diameter distances between source and lens, lens and observer, and source and observer are  $d_{ds}$ ,  $d_d$  and  $d_s$  respectively. From Fig. 5.2 we see that

$$\vec{\beta}d_s = \vec{\theta}d_s - \vec{\alpha}d_{ds}, \quad (5.11)$$

or in terms of the distance  $\vec{\eta} = d_s \vec{\beta}$  between the source and the optical axis,

$$\vec{\eta} = \frac{d_s}{d_d} \vec{\xi} - d_{ds} \vec{\alpha}(\vec{\xi}). \quad (5.12)$$

It is convenient to use the *reduced deflection angle*

$$\vec{\alpha}'(\vec{\theta}) = \frac{d_{ds}}{d_s} \vec{\alpha}(\vec{\theta} d_d), \quad (5.13)$$

by which the position of the source and the image(s) can be related through the simple equation

$$\vec{\beta} = \vec{\theta} - \vec{\alpha}'(\vec{\theta}). \quad (5.14)$$

Equations (5.11), (5.12) and (5.14) are different representations of the *lens equation*. It can be rewritten in dimensionless form by introducing a length scale  $\xi_0$  in the lens plane and a corresponding length scale  $\eta_0 = \xi_0 d_s / d_d$  in the source plane. With the help of these, we define the dimensionless vectors

$$\vec{x} = \vec{\xi}/\xi_0 \quad \text{and} \quad \vec{y} = \vec{\eta}/\eta_0. \quad (5.15)$$

In terms of  $\vec{x}$  and  $\vec{y}$  the lens equation takes the form

$$\vec{y} = \vec{x} - \hat{\vec{\alpha}}(\vec{x}), \quad (5.16)$$

where

$$\hat{\vec{\alpha}}(\vec{x}) = \frac{d_d}{\xi_0} \vec{\alpha}'\left(\frac{\xi_0 \vec{x}}{d_d}\right) = \frac{d_d d_{ds}}{d_s \xi_0} \vec{\alpha}(\vec{\xi}_0 \vec{x}) \quad (5.17)$$

is called the *scaled deflection angle*. The length scale  $\xi_0$  is for the present completely arbitrary. When considering a specific lensing situation, it can be chosen such that the lens equation is the simplest.

## The magnification factor

The flux of the image of an infinitesimal source is the product of its surface brightness and the solid angle it subtends on the sky. Since the photon number is conserved, gravitational light deflection preserves surface brightness [35]. However, gravitational lensing changes the apparent solid angle of a source, thereby affecting the flux of the image. The flux

received from a lensed source is therefore changed in proportion to the ratio between the area of the image and the source,

$$\text{magnification} = \frac{\text{image area}}{\text{source area}}. \quad (5.18)$$

Denoting the *magnification factor*  $\mu$  and the solid angles of the image and the source  $d\omega$  and  $d\omega'$ , respectively, we obtain

$$\mu = \frac{d\omega}{d\omega'}. \quad (5.19)$$

Defining the *magnification tensor*  $\mathcal{M}$  by

$$\mathcal{M} := \frac{d\vec{x}}{d\vec{y}}, \quad (5.20)$$

we can write the magnification factor as

$$\mu(\vec{x}) = \det \mathcal{M}(\vec{x}). \quad (5.21)$$

Note that the magnification factor can be either positive or negative. The corresponding images are said to have positive or negative parity, where the parity of an image determines its orientation relative to that of the unlensed source.

## 5.4 Is it a good thing?

Gravitational lensing can been used to increase our knowledge of the universe in a number of ways:

- Since lensing depends on the distribution of mass within the lens, it can be used to obtain information on individual lenses. Specifically, since it depends *only* on the distribution of mass, i.e., not the type of matter, it can be used to obtain information on the distribution of DM in galaxy and galaxy cluster halos (**Paper III**).
- The statistics of gravitational lensing can be used to put limits on cosmological parameters, in particular the cosmological constant. Also, the time delay in multiple image systems can be used to put limits on the Hubble constant and the energy densities of the universe [15].
- The magnification can be used to detect and study very faint objects, which would otherwise escape detection. In this way, lenses can be used to enhance the power of telescopes.

## Is it always a good thing?

In an inhomogeneous universe, sources may be magnified or demagnified with respect to the case of a homogeneous universe with the same average energy density. This is because the majority of light-rays will travel far from all matter clumps, effectively sensing a smaller average density and thus be demagnified (cf. the DR distance) whereas light-rays passing near, e.g., a galaxy will be magnified. In the case of point-mass lenses, we have seen [Eq. (5.10)] that deflection angles are very small. Using Eq. (5.21), we can compute the magnification caused by a point-mass as

$$\mu = \left[ 1 - \left( \frac{\xi_0}{\xi} \right)^4 \right]^{-1}, \quad (5.22)$$

where  $\xi_0$  is a typical length scale of the system that depends on the mass of the lens and the distances between the lens, the source and the observer. It is obvious that, even though deflection angles are small, magnifications can be very large. In fact,  $\mu \rightarrow \infty$  when  $\xi \rightarrow \xi_0$ . As we will see, this gravitational lensing effect might turn out to be a *bad* thing for certain types of observations. Specifically, we will study how this effect might become of importance when trying to determine cosmological parameters using observations of SNe at high redshifts (**Paper IX**).

## 5.5 Gravitational lensing in SNOC

A detailed account of the implementation of gravitational lensing effects in SNOC can be found in **Paper I** and **VIII**. Here we will summarise the main points of interest.

We use the method proposed by Holz and Wald [19] where lensing effects are calculated by studying the amount of focusing of light-rays whereas the deflection of the light-ray is not taken into account. It is thus well-suited to situations where magnification effects are of primary interest.

We first select a FL background geometry and account for inhomogeneities by specifying matter distributions in cells which have an average energy density equal to that of the underlying FL model.<sup>3</sup> The light-ray

---

<sup>3</sup>In that respect, we neglect another possible influence of inhomogeneities on observed luminosities; that the overall expansion rate of the universe is affected by the inhomogeneities, see [6].

is traced backwards to the desired redshift by being sent through a series of cells, each time with a randomly selected impact parameter with respect to the matter distribution in the cell. Between each cell, the FL background is used to update the scale factor and the expansion rate. The focusing of the light-ray is computed by integrating the geodesic deviation equation (3.26) through each cell, see **Paper I** and Appendix B. By using Monte-Carlo techniques to trace a large number of light-rays, statistics for the apparent luminosity of sources at random lines-of-sight can be obtained.

### Multiple images

The Holz & Wald method is restricted to the study of infinitesimal light-beams, making it impossible to keep track of multiple images from the same source. This poses no problem when the time delay or spatial separation between images is big enough to allow observational separation (as in the case of galaxy mass lenses). However, if image separation is not observationally feasible and we want to consider the total flux from a source, we need to compensate for multiple images. This topic is discussed in Sec. 10 of **Paper I**. It is also possible to obtain information on multiple image systems where images are separable, see Sec. 5.1.4 in **Paper VIII**.

## 5.6 Results

The effect of gravitational lensing on Type Ia SN measurements is to cause a dispersion in the Hubble diagram. In Fig. 5.3 we compare the dispersion due to gravitational lensing with the intrinsic dispersion and the typical measurement error for Type Ia SNe. In the upper left panel, we show an ideal Hubble diagram with no dispersion and in the upper right panel we have added the dispersion due to lensing (lens) in a universe with 20 % compact objects and 80 % smooth DM halos. Comparing with the panel in the lower left where the intrinsic dispersion (intr) and measurement error (err) have been included, we see that the effects become comparable at a redshift of unity. In the lower right the (most realistic) case with intrinsic dispersion, measurement error and lensing dispersion is plotted.

Of course, the additional asymmetric dispersion caused by gravitational lensing will be a source of systematic error in the cosmological

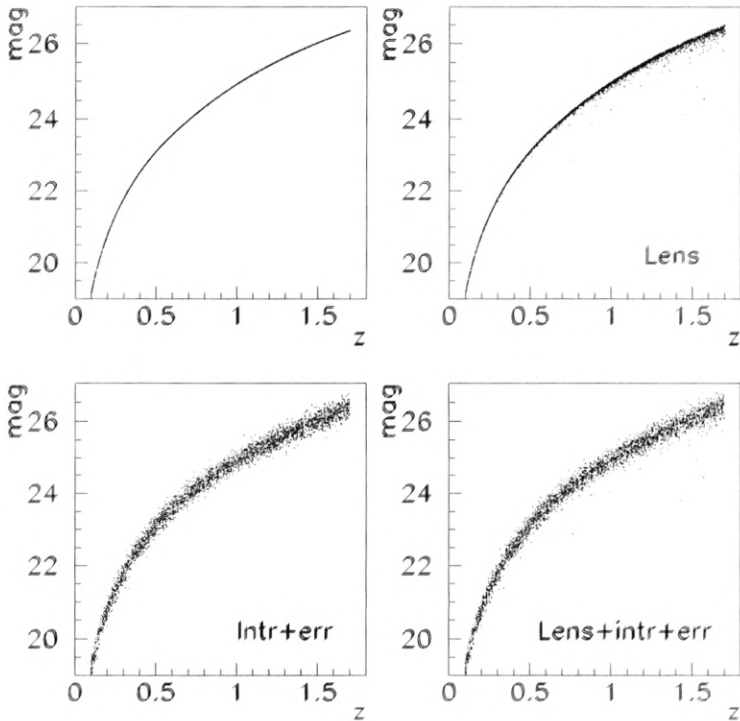


Figure 5.3: A comparison of the dispersion due to lensing (upper right) and the measurement error and intrinsic dispersion of Type Ia SNe (lower left).

parameter determination with Type Ia SNe. However, a possible virtue of lensing is that the distribution of luminosities might be used to obtain some information on the matter distribution in the Universe, e.g., to determine the fraction of compact DM in our Universe. These two competing effects have been the main points of interest in the accompanying papers concerned with gravitational lensing.

In **Paper I** the Holz & Wald method for calculating gravitational lensing effects is generalised in several ways: First, the matter content is allowed to consist of several different types of fluids, also with non-vanishing pressure. Second, besides lensing by simple point-masses and

singular isothermal spheres (SIS) with a fixed mass, the density profile based on N-body simulation results proposed by Navarro, Frenk & White (NFW), as well as a distribution of galaxy masses is treated.

In Fig. 5.4, the luminosity distributions for 10 000 sources at redshift  $z = 2$  in a  $\Omega_M = 0.3$ ,  $\Omega_\Lambda = 0.7$  universe is shown. The full line corresponds to the point-mass case; the dashed line is the distribution for SIS halos, and the dotted line is the NFW case. The magnification zero point is the filled-beam value. Figure 5.4 indicates that the (unlikely) case of having a dominant part of the DM distributed in the form of very compact objects can be distinguished from halo models with DM distributed smoothly, if a sufficient number of SNe can be detected at large redshifts. The similarities in the luminosity distribution obtained with SIS and NFW halos indicate that these cases are difficult to distinguish. However, this has the advantage that, unless a major fraction of the DM is in compact objects, it should be possible to give quite robust predictions for the magnifications of Type Ia SNe over a broad range of reasonable halo models.

In this paper we also derive analytical fitting formulas for the probability distribution of the deviations from filled-beam magnitudes induced by SIS and NFW lenses for different cosmologies and redshifts. These could be used to refine the cosmological parameters estimation as well as deducing the mass distribution in galaxy halos by studying the residual magnitude distributions in future high-redshift searches. This paper was the starting-point for the simulation package SNOC.

One of the first applications of SNOC was the preliminary investigation in **Paper II** where it was showed how a sample of 100 Type Ia SNe at  $z \simeq 1$  can be used to discern between the cases of all DM in compact objects or smooth DM halos.

In Fig. 5.5, the luminosity distributions for 10 000 sources at redshift  $z = 1$  in a  $\Omega_M = 0.3$ ,  $\Omega_\Lambda = 0.7$  universe is shown, including an intrinsic luminosity dispersion of the sources with  $\sigma_m = 0.16$  mag. The full line corresponds to the point-mass case; the dashed line to SIS halos, and the dotted line to NFW halos.

Using the Kolmogorov-Smirnov test to compare simulated experiment data sets with simulated reference samples it was found that for 98 % of the simulated experiments, we were able to rule out a point-mass distribution with a 99 % confidence level. However, in 1 % of the experiments, the halo distribution was erroneously ruled out with the same confidence

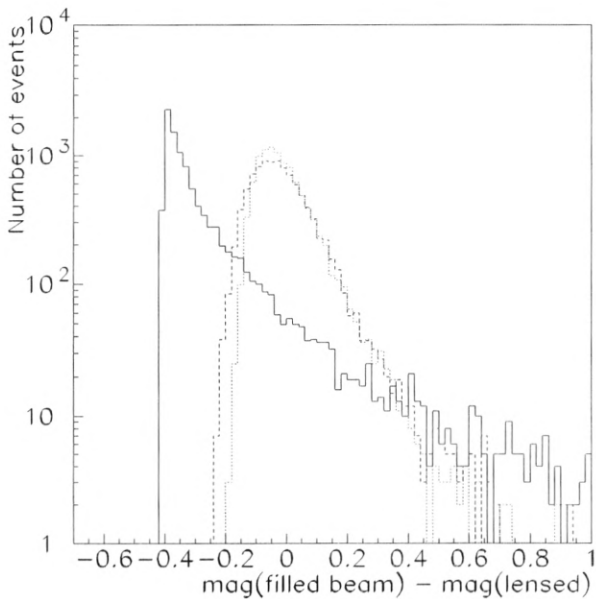


Figure 5.4: Luminosity distributions for 10 000 sources at redshift  $z = 2$  in a  $\Omega_M = 0.3$ ,  $\Omega_\Lambda = 0.7$  universe. The magnification zero point is the filled-beam value. The full line corresponds to the point-mass case; the dashed line is the distribution for SIS halos, and the dotted line is the NFW case.

level. For a similar sample containing 200 SNe, the confidence level was increased to 99.99 %.

Elaborating the method employed in **Paper II**, it was showed in **Paper III** how data from one year's operation of the proposed SNAP satellite can be used to pin down the fraction of DM in compact objects to  $\lesssim 5\%$  accuracy. It has previously been shown [34] that it should be possible to determine the fraction of compact objects to 20 % accuracy with 100–400 Type Ia SNe at  $z = 1$ . In this analysis, simulated magnification probability distribution functions (pdf) for large scale structure are combined with analytical pdf's for lensing by compact objects to obtain combined pdf's for different fractions of compact objects. The accuracy to which it is possible to determine  $f_p$  is then estimated by studying the covariance matrix.

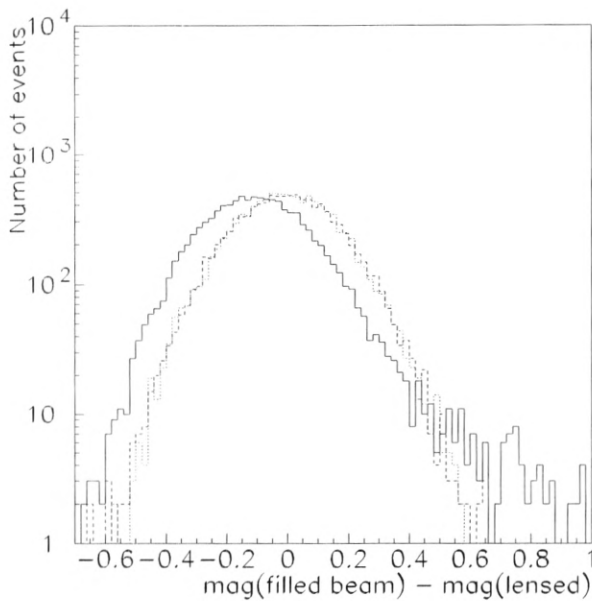


Figure 5.5: Luminosity distributions for 10 000 sources at redshift  $z = 1$  in a  $\Omega_M = 0.3$ ,  $\Omega_\Lambda = 0.7$  universe. This is the basically the same situation as depicted in Fig. 5.4, only at a lower redshift and with an added intrinsic luminosity dispersion of the sources with  $\sigma_m = 0.16$  mag. (corresponding to the case of Type Ia SNe).

In **Paper III**, a full Monte-Carlo method is used for the same type of analysis. Using SNOC, we created large SN data sets with the fraction of compact objects ranging from 0 to 40 % to be used as reference samples. In Fig. 5.6 the reference samples for 0 % (full line), 20 % (dashed line) and 40 % (dotted line) compact objects is plotted. In the lower panel we have added the intrinsic dispersion and measurement error,  $\sigma_m = 0.16$  mag.

We also created a large number of simulated one-year SNAP data sets with 6, 11 and 21 % compact objects to serve as experimental samples. By comparing each generated experimental sample with our high-statistics reference samples using the Kolmogorov-Smirnov test, we were able to determine the fraction of compact objects with a one-sigma error less than 5 %. If the intrinsic dispersion and measurement error can be further

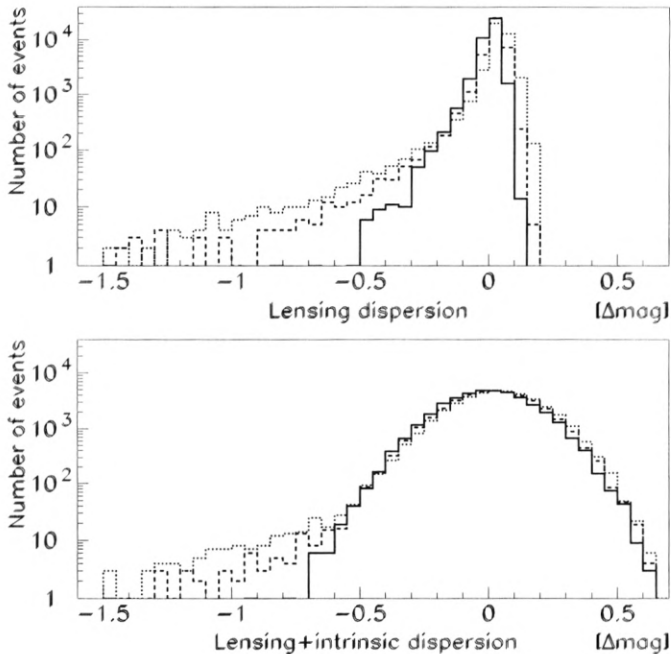


Figure 5.6: Magnitude dispersion of reference samples for 0 % (full line), 20 % (dashed line) and 40 % (dotted line) compact objects. The bottom panel includes a gaussian smearing,  $\sigma_m = 0.16$  mag.

reduced, the accuracy can be improved even further.

Since Monte-Carlo methods are used, we do not need to parametrise the pdf's for different fractions of compact objects, nor bin any data in order to perform the statistical analysis. A drawback with using SNOC as compared to the analysis in [34] is that we do not include the effects from large scale structure in our lensing calculations. On the other hand, we are able to do very detailed modeling of the structure up to galaxy scales. A possibility would be to combine the pdf's from large scale structure with the pdf's from galaxy scale structure that we obtain from our Monte-Carlo simulations. Such an analysis has not yet been performed.

Even though lensing can be very useful when it comes to the investigation of DM clustering properties, it will still have the less desirable effect of introducing a bias in the Hubble diagram when doing precision

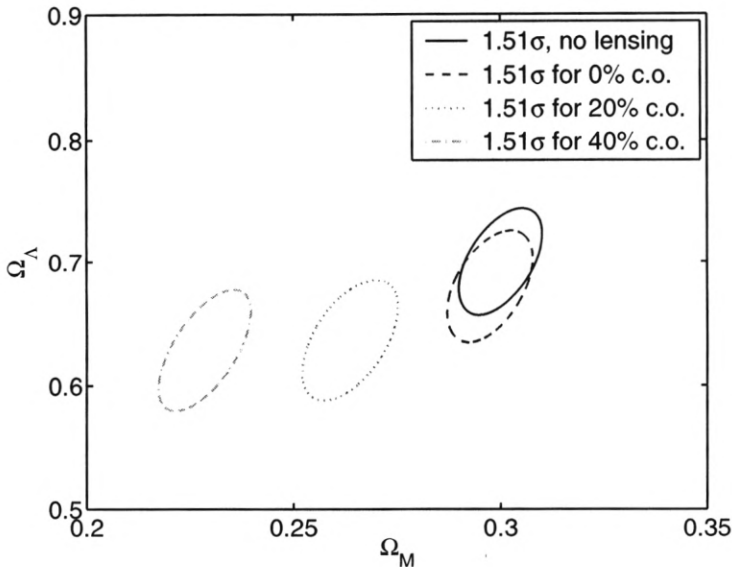


Figure 5.7:  $1.51\sigma$  confidence contours (corresponding to the 68 % level for two parameters) for three-parameter  $\chi^2$ -fits of the cosmological parameters ( $\Omega_M, \Omega_\Lambda, \mathcal{M}$ ). The dashed contour shows the fit when a NFW halo model has been applied, and the dotted and dash-dotted contours represent different fractions of compact objects (c.o.) in the dark matter model.

cosmology with Type Ia SNe.

In Eq. (4.5) it was shown how the apparent magnitude of a standard candle is related to the cosmology dependent luminosity distance. Given a data set of Type Ia SN magnitudes and redshifts, the usual procedure is to make a  $\chi^2$ -fit of, e.g.,  $\Omega_M, \Omega_\Lambda$  and  $\mathcal{M}$  assuming a gaussian dispersion in the magnitudes. Since gravitational lensing will induce an asymmetry in the magnitude distribution, the use of a gaussian pdf can, e.g., yield a too low value of  $\Omega_M$  as is shown in Fig. 5.7 where  $1.51\sigma$  confidence contours (corresponding to the 68 % level for two parameters) for the three-parameter  $\chi^2$ -fit of  $(\Omega_M, \Omega_\Lambda, \mathcal{M})$  is shown. The fits are based on simulated samples of 2300 SNe uniformly distributed in the redshift interval  $0 < z < 2.2$  with different gravitational lensing models. The dashed contour shows the fit when a NFW halo model has been applied, and the dotted and dash-dotted contours represent different fractions of compact

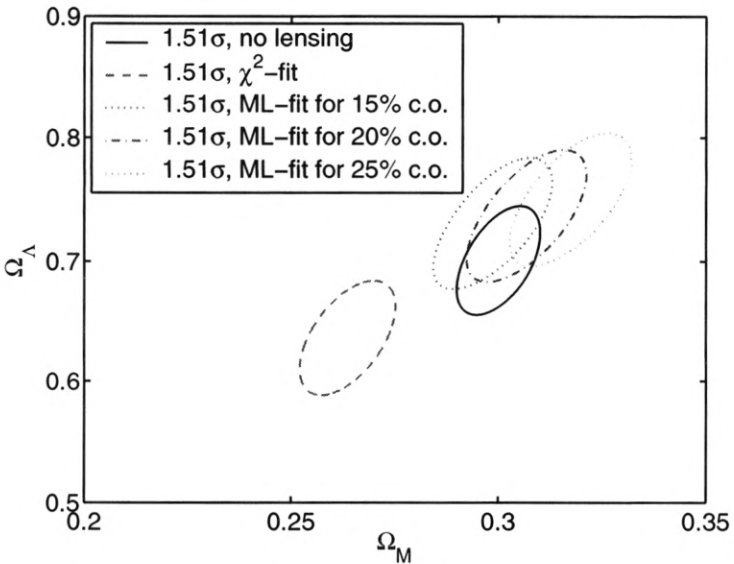


Figure 5.8: The solid contour shows the  $\chi^2$ -fit result when lensing effects are absent and the dashed contour is the case for a dark matter model with 20 % compact objects and 80 % NFW halos if lensing effects are neglected in the fit. The dash-dotted contour shows the result obtained with the same sample when the correct pdf is used. The two dotted contours shows the result when an incorrect value ( $\pm 5\%$ ) of the fraction of compact objects (c.o.) is assumed.

objects.

In **Paper IX**, it is showed how one can avoid a bias in the cosmological parameter determination by performing a maximum likelihood analysis with the correct pdf. Since lensing effects are similar for different smooth dark matter halo distributions but sensitive to the fraction of the matter density in compact objects,  $f_p$  (see **Paper III**), we can parametrise the amount of lensing with  $f_p$ . We use SNOC to obtain simulated samples of the intrinsic dispersion and gravitational lensing effects of Type Ia SNe and parametrise the pdf's for different fractions of compact objects and redshifts with a shifted gaussian with a high magnification tail.

In Fig. 5.8 we show the 68 % confidence contours for one specific experimental realisation using the parametrised pdf's for different lensing models. The dash-dotted contour corresponds to the case where we as-

sume that we know  $f_p$  exactly and the two dotted contours show the bias corresponding to a 5 % error in the determination of  $f_p$ . It is obvious that if  $f_p$  can be determined with < 5 % accuracy, it should be possible to reduce the bias due to lensing significantly, as compared to the case where the magnitudes are assumed to be gaussian distributed. Since such an error is within reach with the SNAP satellite, we conclude that it should be possible to correct for lensing bias in an effective way for future SN surveys.

The possible impact of lensing of a single SN is studied in **Paper IV**, where gravitational lensing effects on the observed luminosity of SN1997ff, a Type Ia SN at  $z \simeq 1.7$ , is investigated. The relative positions and redshifts of galaxies lying in the proximity (closer than 10 arcseconds) of the line-of-sight to SN1997ff are obtained from the Hubble Deep Field North. We model the matter distribution of the galaxies as truncated isothermal spheres and estimate the masses and velocity dispersions of the lensing galaxies from the measured luminosities.

In Fig. 5.9, the combined magnification from all lensing galaxies is given as a function of the normalisation of the mass of the galaxies,  $m_*$ , which is a very uncertain parameter. The discontinuities are due to the fact that the truncated halos get bigger when we increase  $m_*$ , and thus the light-ray will pass through a larger number of halos with an increased magnification as an effect. Of course, this effect is unphysical in the sense it is sensitive to the specific modeling of the halos but it serves as an important reminder of the model dependence of gravitational lensing effects. The conclusion in **Paper IV** is that very detailed, individual modeling of the lensing galaxies is necessary to make robust predictions of the gravitational lensing of SN1997ff and that with the current knowledge of the lensing galaxies, it is possible to obtain a wide range of magnifications by varying the galaxy model parameters.

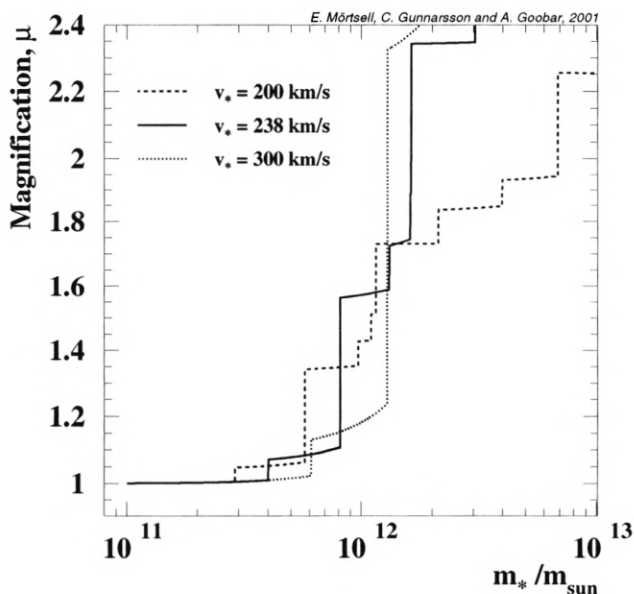


Figure 5.9: The magnification,  $\mu$ , of SN1997ff as a function of the mass normalisation,  $m_*$ , for three different values of the typical velocity dispersion,  $v_*$ , of the foreground galaxies.

# Chapter 6

## Dust

The absorption of light from high redshift supernovae by dust is investigated with special emphasis on a possible homogeneous “grey” dust component.

### 6.1 Introduction

Looking at the sky, one can see dark lanes across the Milky Way. These dark patches were once attributed to a deficiency of stars, but are now known to be regions obscured by dust. The extinction is believed to be caused by small particles, or grains, that absorb and scatter the light from background stars.

Observational evidence for extinction due to dust comes from several different phenomena. First, the extinction tends to be more severe at shorter wavelengths, causing objects to look redder. Second, it is possible to identify specific spectroscopic features in the extinction, corresponding to different dust constituents. Also, the absorbed light is reradiated in the infrared and the scattered light can be seen as reflection nebulae if the dust cloud is close enough to some bright light source.

In this thesis we investigate the role of dust absorption in the context of SN observations, concentrating on a possible intergalactic, homogeneous dust component with rather achromatic extinction properties.

## 6.2 Dust and Type Ia supernovae

When studying the effect of dust extinction on SN observations, we need to consider at least four different dust environments:

1. A host galaxy dust component
2. Dust in galaxies between the source and the observer
3. A homogeneous intergalactic dust component
4. Milky Way dust

If there is a significant homogeneous component (3) that causes a very small amount of reddening (“grey” dust), one can get an effect similar to that of a cosmological constant (or some other energy component with negative pressure permeating all through space) in the respect that high redshift sources will look fainter. This kind of dimming due to an intergalactic grey dust component has been proposed as an alternative explanation for the observed reduction of SN fluxes at high redshifts [1, 2].

We have very little knowledge of the properties and abundances of intergalactic dust, but the fact that the intergalactic medium is metal rich indicates that metal can be effectively transferred from the galaxies in which it forms to the intergalactic space. It has been argued [2] that it is difficult to remove metallic gas from galaxies without also removing dust. Thus, the intergalactic dust can be assumed to be ejected from galaxies, perhaps driven by radiation pressure.

A short calculation shows what kind of dust density is needed in order to get the same attenuation as the difference between two different cosmologies. We can write [see, e.g., Eq. (6.8)]

$$\frac{d(\Delta m_d)}{dz} = \text{const} \cdot \frac{\rho_{\text{dust}}(z)}{(1+z)H(z)}, \quad (6.1)$$

where the subscript “d” denotes attenuation due to dust. Since  $m(z) = 5 \log_{10} d_L(z) + \text{const}$ , we get

$$\Delta m_c = 5 \log_{10} \left[ \frac{d_L(1, z)}{d_L(2, z)} \right], \quad (6.2)$$

where the subscript “c” denotes magnitude difference between different set of values for the cosmological parameters, represented by arguments

1 and 2. Thus,

$$\frac{d(\Delta m_c)}{dz} = \text{const} \cdot \left[ \frac{d_L(1, z)}{d_L(2, z)} \right]^{-1} \frac{d}{dz} \left[ \frac{d_L(1, z)}{d_L(2, z)} \right]. \quad (6.3)$$

This shows that in order to get an attenuation due to dust of the same magnitude as the difference in observed magnitudes between cosmologies 1 and 2, we need a homogeneous grey dust component with physical density

$$\rho_{\text{dust}}(z) = \text{const} \cdot (1 + z) H(z) \left[ \frac{d_L(1, z)}{d_L(2, z)} \right]^{-1} \frac{d}{dz} \left[ \frac{d_L(1, z)}{d_L(2, z)} \right]. \quad (6.4)$$

In the upper panel of Fig. 6.1, we show the magnitude difference between a  $\Omega_M = 0.3, \Omega_\Lambda = 0.7$  universe and  $\Omega_M = 1$  and  $\Omega_M = 0.3$ , respectively. The comoving dust density needed to mimic this effect is shown (in arbitrary units) in the lower panel. It can be seen, that in order to get the same dimming due to dust as in a vacuum energy dominated cosmology, we need dust to be continuously expelled from galaxies (or created in the intergalactic medium) from a redshift of  $z \sim 1$ .

Since measurements of the CMBR anisotropies indicates that the universe is close to flat [23, 37, 28], while observations of large scale structure [25] and galaxy cluster evolution [4] gives  $\Omega_M \sim 0.3$ , it is unlikely that the faintness of Type Ia SNe is caused by dust extinction only, see also Ch. 4. However, we still need to consider the possibility that grey dust is capable of biasing the results from Type Ia SN observations, with particular attention paid to the frequency dependence of the effect.

### 6.3 Dust model

It is very difficult to constrain the properties of dust down to some specific grain model since several models are able to explain the observational data mentioned in Sec. 6.1. Therefore, there are big uncertainties regarding both the composition and size distribution, as well as the optical properties of interstellar grains in general and intergalactic grains in particular.

However, dust grains are believed to span a large range of sizes, from very small dust grains consisting of single small molecules to micron size particles. Also, from the spectral features of the dust extinction, it appears that approximately 50 % of the grain mass is in silicate grains and 50 % in carbon grains.

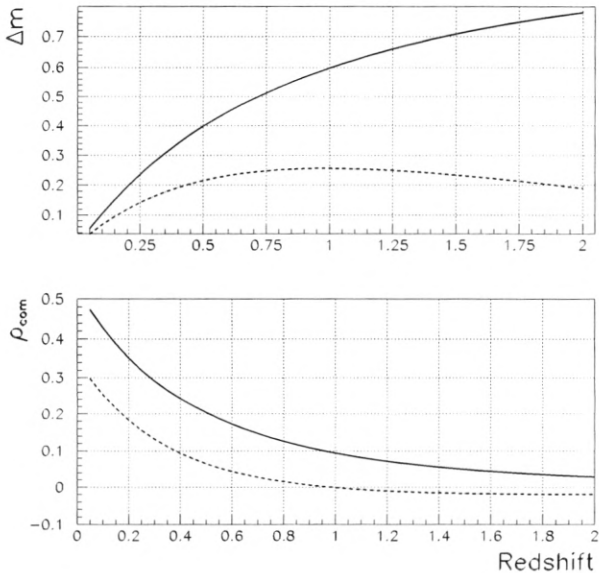


Figure 6.1: The upper panel shows the magnitude difference between a  $\Omega_M = 0.3, \Omega_\Lambda = 0.7$  universe and  $\Omega_M = 1$  (full line),  $\Omega_M = 0.3$  (dashed line). The lower panel shows the comoving dust density (in arbitrary units) needed to mimic a  $\Omega_M = 0.3, \Omega_\Lambda = 0.7$  universe if the true values are  $\Omega_M = 1$  (full line),  $\Omega_M = 0.3$  (dashed line).

There are arguments to why the intergalactic dust should have different properties than galactic dust [2]. If the intergalactic dust is produced in, and expelled from starburst galaxies, large grains are preferentially ejected since radiation pressure favour high opacity, less reddening grains. Also during the expulsion process, small grains may be destroyed. Since the smallest grains cause the most severe reddening, the intergalactic dust may be very grey in the respect that the extinction will be rather achromatic.

The minimal grain size surviving expulsion have been computed to be  $a_{\min} \sim 0.05 \mu\text{m}$  which is an interesting number since it can be shown that if the minimum grain size is  $a_{\min} > 0.1 \mu\text{m}$ , then the dust would be too grey to violate any current reddening constraints, even for dust densities high enough [ $\Omega_{\text{dust}}(z = 0.5) \approx 4 \times 10^{-5}$ ] to cause a dimming comparable

to the one caused by a cosmological constant [2].

For any given model, it is important to characterise the frequency dependence of the extinction in order to be able to correct the observations and control any unwanted bias. We use a dust model consisting of silicon grains and carbon grains in the form of crystalline graphite. The grains have a size distribution

$$\frac{dn}{da} \propto a^{-3.5} \quad (6.5)$$

with  $a_{\max} \approx 250$  nm [21]. The Draine & Lee model consists of silicate and graphite spheroids with the above distribution in size and synthesised dielectric functions to give the absorption cross-section [10]. This model is widely used and captures the essential features of dust absorption. The graphite grains are found to give very little reddening, i.e., the reddening is mostly due to the silicate. We assume that the intergalactic dust population can be described by a Draine & Lee model where the smaller grains are absent, thereby causing very little reddening.

Based on empirical evidence, it has been shown that the frequency dependence of the dust obscuration along different lines-of-sight can be described by an average extinction law  $A(\lambda)$  depending on one parameter,  $R_V$ , only [8]. The reddening parameter  $R_V$  is defined by

$$R_V = \frac{A(V)}{E(B - V)}, \quad (6.6)$$

where  $A(V)$  is the extinction integrated over the  $V$  band and

$$E(B - V) = (B - V) - (B - V)_i \quad (6.7)$$

with  $(B - V)_i$  being the intrinsic (unobscured) colour. Thus, if we know the difference between the intrinsic and the observed colour  $E(B - V)$ , we can correct for the dust extinction, assuming some value for  $R_V$ .

The observed value of  $R_V$  varies markedly between galaxies,  $1.5 < R_V < 7.2$ . In the Milky Way, we have  $3 < R_V < 6$ . As previously noted, the absence of small dust grains will decrease the wavelength dependence of extinction. In the adopted parametrisation this corresponds to higher values of  $R_V$ . Thus, the optical properties, of which  $R_V$  is the most important for our applications, depend on the value chosen for the small-size cut-off  $a_{\min}$  in the power-law size distribution. We use  $a_{\min}$  between 0.08 and 0.12  $\mu\text{m}$ , corresponding roughly to  $R_V$  between 5.5 and 9.5.

With a specific average extinction law  $A(\lambda, R_V)$ , we can calculate the attenuation due to dust  $\Delta m_d$  at observed wavelength  $\lambda_o$  for a given emission redshift  $z$  as

$$\Delta m_d(z, \lambda_o) = -2.5 \log_{10} \exp \left[ -C \int_0^z \frac{\rho_{\text{dust}}(z') A(\lambda_o/(1+z'), R_V) dz'}{(1+z') H(z')} \right], \quad (6.8)$$

where  $\rho_{\text{dust}}(z)$  is the physical dust density at redshift  $z$  and  $H(z)$  is given by Eq. (3.51). The normalisation constant  $C$  is related to the overall magnitude of the extinction.

## 6.4 Dust in SNOC

The simulation programme SNOC can be used to perform the integral in Eq. (6.8) numerically by following individual light-paths through a large number of cells containing galaxies and intergalactic dust. Through each cell the background cosmology, the wavelength of the photon and the dust density are updated, and the contributions from each cell added. The model is approximately valid also for a patchy dust distribution, as long as the number of intersected patches is large enough, i.e.,  $1/\sqrt{N} \ll 1$  where  $N$  is the number of dust clouds intersected by the light-ray.

It is also possible to simulate extinction due to dust in the host galaxies of SNe and in intervening galaxies along the line-of-sight.

The absorption in the host galaxy will be different for different SN types. This is because core collapse SNe occur in late type, starforming, dusty galaxies whereas Type Ia's can occur in any type of galaxy. In SNOC, we let the probability for a SN to occur in a specific galaxy be proportional to the galaxy luminosity in order to allow for SNe to be more common in star-rich, luminous galaxies. We also assume that the amount of dust and the SN rate is proportional to the luminosity, i.e., the amount of stars in the galaxy. The dust distribution in late type galaxies is modeled as a double exponential disc. For further reference regarding dust and SN distribution in host galaxies, see [18]. After determining the dust distribution and SN position in the galaxy, we assume a random inclination of the disc and integrate the absorption along the path of the light-ray through the disc.

The extinction due to dust in the case of close encounters of intervening galaxies is calculated by first selecting the galaxy type and mass

in each cell using Monte-Carlo methods. If the galaxy is a spiral, the absorption due to the dusty disc is computed (if the light-ray passes it). Equivalent to the case of host galaxies, we model the dust distribution in intervening spiral galaxies by a double exponential disk with random inclination.

## 6.5 Results

As already mentioned, to avoid observational constraints on reddening, any significant, intergalactic dust component must mainly consist of large dust grains. However, even large dust grains will cause reddening, and going to higher redshift would make it possible to observe this effect.

In **Paper VI**, the differential extinction for high-redshift sources caused by intergalactic dust along the line-of-sight is investigated. It is shown how future observations of Type Ia SNe up to  $z \sim 2$ , e.g., by the SNAP satellite, will allow the measurement of the properties of intergalactic dust and thus allow tests for obscuration affecting the measurements of high- $z$  SNe.

This is done by simulating scenarios where the extinction due to dust introduces a bias in the Hubble diagram in excess of  $\delta m=0.02$  for  $z \leq 2$  (the target for systematic uncertainties for SNAP). Fig. 6.2 shows the colour extinction (at maximum intensity) in  $V - J$ ,  $R - J$  and  $I - J$  for a normal Type Ia SN as a function of redshift for  $R_V=5.5$  (left panel) and  $R_V=9.5$  (right panel).<sup>1</sup> The dust density is given by

$$\rho_{\text{dust}} = \begin{cases} \rho \propto (1+z)^3 & z < 0.5 \\ \rho = \text{const} & z > 0.5 \end{cases}$$

That is, the comoving density increases with cosmic time until  $z = 0.5$  from which it is constant. It can be seen that the average  $V - J$ ,  $R - J$  and  $I - J$  colours of normal Type Ia SNe are significantly different with and without the grey dust component. More specifically, with 1% relative spectrophotometric accuracy or broad-band photometry in the wavelength interval 0.7–1.5  $\mu\text{m}$ , one should be able to measure the extinction caused by grey dust down to  $\delta m = 0.02$  magnitudes, the error target for SNAP.

---

<sup>1</sup>All the broad-band filters and spectroscopy wavelength scales are in the observer's frame.

If the faintness of Type Ia SNe is to be attributed to grey dust as opposed to a dark energy component with negative pressure, a colour extinction  $E(R - J) \gtrsim 0.1$  mag is to be expected for sources at  $z \sim 0.5$ . This is possible to test with current ground based facilities and thus it should be possible to distinguish between extinction or a cosmological origin for the faintness of Type Ia SNe at  $z \sim 0.5$ .

In **Paper VI**, we have also examined the probability of extinction of Type Ia SNe from intervening galaxies and host galaxies. Extinction from intervening galaxies is a relatively small effect, affecting less than 1% of sources at  $z = 1$  in a non-negligible way. Extinction in the host galaxy is potentially a more serious problem but in general we expect dust in galaxies to have  $R_V \sim 3$ , causing enough reddening to be able to control the effect with high accuracy spectrophotometry.

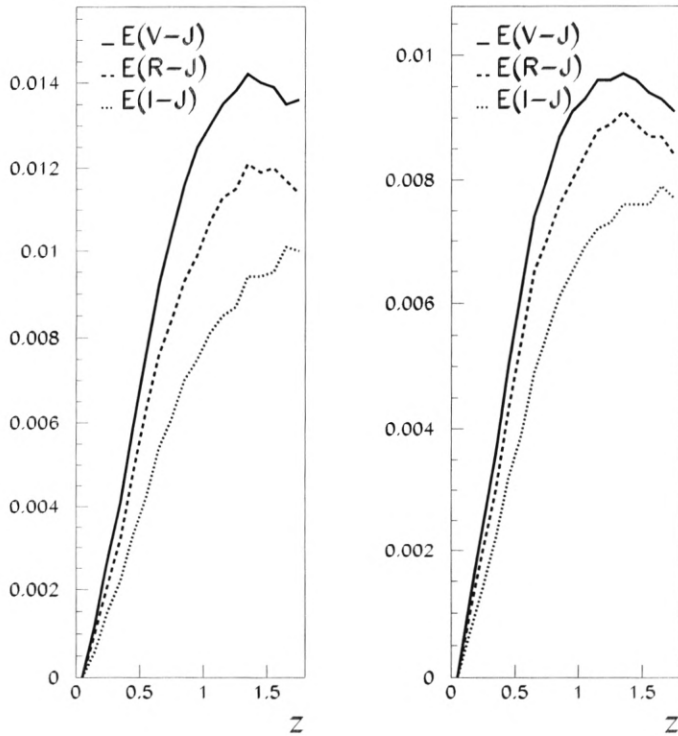


Figure 6.2: Colour extinctions  $E(V - J)$ ,  $E(R - J)$  and  $E(I - J)$  for Type Ia SNe for  $R_V=5.5$  (left panel) and  $R_V=9.5$  (right panel) with the dust density adjusted to generate about 0.02 mag dimming in the observed band corresponding to the restframe B-band magnitude from a source at  $z \sim 2$ .



# Chapter 7

## Photon-axion oscillations

The possibility of photons oscillating into a very light axion and its effects on supernova observations are investigated.

### 7.1 Introduction

In this chapter we investigate an exotic alternative explanation of the faintness of high redshift SNe, namely that photons propagating in intergalactic magnetic fields can oscillate into very light axions. The hypothetical axion is a consequence of certain extensions of the standard model and the conversion of photons into axions will make distant SNe look dimmer and may produce effects very similar to that of a dark energy component with a negative equation of state, e.g., the cosmological constant. The presence of a significant component of dark energy has recently been independently inferred from other cosmological tests (see Ch. 4), therefore the proposed photon-axion mixing does not remove the need for such a component, but its equation of state need not be as close to that for a cosmological constant as is the case without oscillations.

### 7.2 The axion

Photons can mix with low mass bosons in the presence of external electromagnetic fields if these particles couple by a two-photon vertex. Since the photon is a spin 1 particle and the axion has zero spin, we need a mixing agent in order to conserve quantum numbers during the process. The

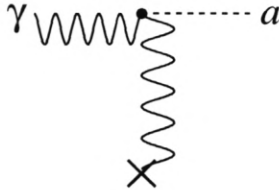


Figure 7.1: The Primakoff conversion between photons and axions in an external electromagnetic field.

mixing agent could be a magnetic field transverse to the propagation direction of the photon. The strength of intergalactic magnetic fields is not well-constrained. This has to do with the fact that the most important observational technique used to trace far-away intergalactic magnetic fields – Faraday rotation measurements of polarised light passing through an ionised medium – require knowledge of the intergalactic electron density,  $n_e$  as well as the field configurations [16]. Thus, only model dependent upper limits are available.

The interaction between the photon and the axion is described by

$$\mathcal{L}_{\text{int}} = \frac{a}{M_a} \vec{E} \cdot \vec{B}, \quad (7.1)$$

where  $a$  is the axion field,  $M_a$  is a mass scale determining the strength of the coupling and  $\vec{E}$  and  $\vec{B}$  are the electrical and magnetic field, respectively. The strength of the coupling is given by

$$M_a \simeq \frac{\pi f_a}{\alpha} \quad (7.2)$$

where  $f_a$  is the decay constant of the axion, or the Peccei-Quinn scale. This coupling allows for the axion decay  $a \rightarrow 2\gamma$  as well as the Primakoff conversion  $a \leftrightarrow \gamma$  in an external electromagnetic field as depicted in Fig. 7.1.

Axions acquire an effective mass,  $m_a$ , by their interactions with gluons inducing transitions to neutral pions. This mass is approximately given by

$$m_a f_a \approx m_\pi f_\pi, \quad (7.3)$$

where  $m_\pi = 135$  MeV is the pion mass and  $f_\pi \approx 93$  MeV its decay constant. This relation should be regarded with caution since the axion

mass depends on the quark mass ratios as well as higher-order corrections which have not been estimated.

Searches for axions have been negative, placing limits on the axion mass and coupling strength. The most important astrophysical limits on  $f_a$  are based on the requirement that the axionic energy loss of stars, e.g., globular cluster stars or the core of SN1987A, is not too efficient. These considerations imply a lower limit on the decay constant  $f_a \gtrsim 10^9$  GeV (corresponding to  $m_a \lesssim 10^{-2}$  eV), indicating that axions, if they exist, are very light and very weakly interacting.<sup>1</sup>

Even though the interaction parameters and the mass of the axion are severely constrained, whether they exist remains an open question with possible far reaching consequences, e.g., the axion could be the missing DM, or as investigated in this thesis, a very light axion could mimic the effect of a dark energy component.

## Axions as dark matter

If axions were strongly interacting, they would have been in thermal equilibrium in the early universe and hence there would be a background of thermal axions. This range ( $f_a \lesssim 10^8$  GeV) is excluded, hence axions are so weakly interacting that they never were in thermal equilibrium, causing large uncertainties in the predicted cosmic axion density.

Keeping this in mind, the energy density contributed by cosmic axions can be estimated to be [29]

$$\Omega_a h^2 \sim \left( \frac{f_a}{10^{12} \text{GeV}} \right)^{1.175}, \quad (7.4)$$

implying that  $f_a \lesssim 10^{12}$  GeV in order not to completely dominate the universe. This corresponds to  $m_a \gtrsim 10^{-5}$  eV.

Thus, there remains an axion window  $10^{-5}$  eV  $< m_a < 10^{-2}$  eV, where axions can exist and provide a significant fraction of the DM. There are a couple of ongoing experiments investigating this mass range [17, 24]. The very light axion investigated in this thesis ( $m_a \approx 10^{-16}$  eV) can therefore not constitute the missing DM. On the other hand, it may mimic a dark energy component when observing high redshift sources.

---

<sup>1</sup>A proposed laboratory experiment to detect axions involves propagating a light-beam through a magnetic field, blocking its way and measuring the transmitted photons due to the axion component penetrating the wall [38].

### 7.3 Oscillations

The conversion probability for photon-axion oscillations can be calculated using a density matrix formalism (see, e.g., [31]) by following light-paths through simulated universes in a Monte-Carlo fashion. Following the notation of [9], we define the mixing matrix as

$$M = \begin{pmatrix} \Delta_{\perp} & 0 & \Delta_M \cos \alpha \\ 0 & \Delta_{\parallel} & \Delta_M \sin \alpha \\ \Delta_M \cos \alpha & \Delta_M \sin \alpha & \Delta_m \end{pmatrix}. \quad (7.5)$$

The different quantities appearing in this matrix are given by

$$\Delta_{\perp} = -3.6 \times 10^{-25} \left( \frac{\omega}{1 \text{ eV}} \right)^{-1} \left( \frac{n_e}{10^{-8} \text{ cm}^{-3}} \right) \text{ cm}^{-1}, \quad (7.6)$$

$$\Delta_{\parallel} = \Delta_{\perp}, \quad (7.7)$$

$$\Delta_M = 2 \times 10^{-26} \left( \frac{B_{0,\perp}}{10^{-9} \text{ G}} \right) \left( \frac{M_a}{10^{11} \text{ GeV}} \right)^{-1} \text{ cm}^{-1}, \quad (7.8)$$

$$\Delta_m = -2.5 \times 10^{-28} \left( \frac{m_a}{10^{-16} \text{ eV}} \right)^2 \left( \frac{\omega}{1 \text{ eV}} \right)^{-1} \text{ cm}^{-1}, \quad (7.9)$$

where  $B_{0,\perp}$  is the strength of the magnetic field perpendicular to the direction of the photon,  $M_a$  is the inverse coupling between the photon and the axion,  $n_e$  is the electron density,  $m_a$  is the axion mass and  $\omega$  is the energy of the photon. The angle  $\alpha$  is the angle between the (projected) magnetic field and the (arbitrary, but fixed) perpendicular polarisation vector. Our standard set of parameter-values is given by

$$\begin{aligned} B_0 &= 10^{-9}(1+z)^2 \text{ G}, \\ M_a &= 10^{11} \text{ GeV}, \\ m_a &= 10^{-16} \text{ eV}, \\ n_e(z) &= 10^{-8}(1+z)^3 \text{ cm}^{-3}, \end{aligned} \quad (7.10)$$

with a 20% dispersion in  $B_0$  and  $n_e$ . The equation to solve for the evolution of the density matrix  $\rho$  is given by

$$i\delta_t \rho = \frac{1}{2\omega} [M, \rho], \quad (7.11)$$

with initial conditions

$$\rho_0 = \begin{pmatrix} \frac{1}{2} & 0 & 0 \\ 0 & \frac{1}{2} & 0 \\ 0 & 0 & 0 \end{pmatrix}. \quad (7.12)$$

The three diagonal elements refer to two different polarisation intensities and the axion intensity, respectively. We solve the system of 9 coupled (complex) differential equations numerically by following individual light-paths through a large number of cells where the strength of the magnetic field and the electron density is determined from predefined distributions and the direction of the magnetic field is random. Through each cell the background cosmology and the wavelength of the photon are updated, as are the matrices  $\rho$  and  $M$ .

## 7.4 Results

In **Paper VII**, the photon-axion conversion probability is calculated using the density matrix formalism described in Sec. 7.3 and its effect on Type Ia SN observations is investigated.

In Fig. 7.2, we show the rest-frame  $B$ -band magnitude attenuation for Type Ia SNe due to photon-axion oscillations for three different values of the electron density in the redshift interval  $0 < z < 2$ , using values for the other input parameters from Eq. (7.10). Each point represents the average value and the error bars the dispersion for ten different lines-of-sight. In the upper panel, we have used  $n_e = 10^{-7} \text{ cm}^{-3}(1+z)^3$ , in the middle panel  $n_e = 5 \times 10^{-8} \text{ cm}^{-3}(1+z)^3$  and in the lower panel  $n_e = 10^{-8} \text{ cm}^{-3}(1+z)^3$ . Note that the effect is not necessarily increasing with increasing redshift. Thus the numerical simulations indicate that in order to get a dimming effect from photon-axion oscillations similar to the one from a cosmological constant (increasing at lower redshifts, saturating at higher), one would need to have an average intergalactic electron density of  $n_e \lesssim 10^{-8} \text{ cm}^{-3}(1+z)^3$ .

In Fig. 7.3, we show the attenuation due to photon-axion oscillations as a function of wavelength for one specific line-of-sight to  $z = 0.5$  for our standard set of input parameter-values. The most dramatic effect is the strong variation of attenuation with photon energy. Therefore, by analysing relatively narrow spectral features of high redshift objects, one should be able to discern between the dimming effect from oscillations and a cosmological constant.

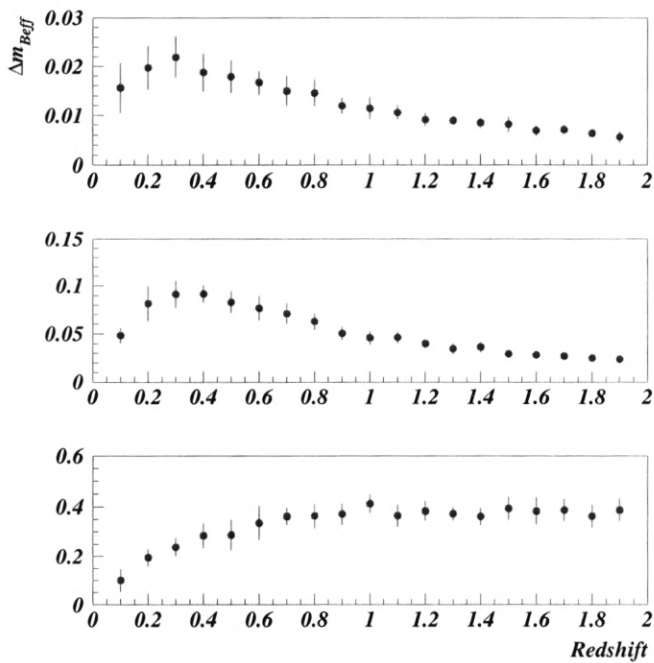


Figure 7.2: The attenuation integrated over the rest-frame  $B$ -band of Type Ia SNe due to photon-axion oscillations with  $n_e = 10^{-7} \text{ cm}^{-3}(1+z)^3$  (upper panel),  $n_e = 5 \times 10^{-8} \text{ cm}^{-3}(1+z)^3$  (middle panel) and  $n_e = 10^{-8} \text{ cm}^{-3}(1+z)^3$  (lower panel). All other parameter-values are given by Eq. (7.10).

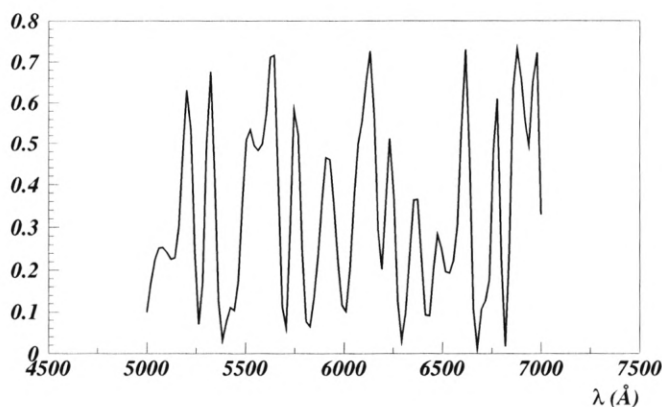


Figure 7.3: The attenuation due to photon-axion oscillations for the standard set of parameter-values [see Eq. (7.10)] as a function of wavelength for a source at redshift  $z = 0.5$ .



# Chapter 8

## Conclusions

The major part of this thesis is concerned with different systematic effects on Type Ia SN observations, including gravitational lensing, dust extinction and photon-axion oscillations.

Photon-axion oscillations are found to be able to mimic the dimming of high redshift SNe caused by a non-zero cosmological constant quite well when integrating over broad-band filters. However, the effect is extremely frequency dependent, inducing a dispersion in the attenuation over wavelength intervals  $\sim 100$  Å of the same order as the integrated attenuation. Thus, by analysing spectra from different high redshift sources it should be possible to control the effect to high accuracy. This has yet to be done.

It is also possible to construct fairly realistic dust density models able to reproduce the observed dimming of high redshift SNe. Once again, the frequency dependence of the effect provides the means of controlling it. Even for very grey dust, there will be some reddening which should be possible to detect and thus control the effects from dust extinction in the Hubble diagram. As of today, the effect cannot be ruled out.

Since gravitational lensing is an achromatic effect, we cannot use any frequency dependence to detect it. A possible signature of gravitational lensing is instead that the distribution of luminosities is modified from the intrinsic gaussian distribution to an asymmetric distribution with a high magnification tail. The induced asymmetry is larger for larger fractions of compact objects in the universe. With large enough statistics, it is possible to determine the fraction of compact objects by studying the luminosity distribution. This information can then be used to reduce the bias in the parameter determination.



## Appendix A

# Gravitational lensing in Newtonian gravity

The deflection angle as computed in Newtonian gravity is often quoted but seldom derived. Therefore, we devote a couple of pages to this calculation.

Let  $\vec{r} = r\hat{r}$  denote the position of the mass particle and  $\vec{F} = F(r)\hat{r}$  be the radial force per unit mass. The equation of motion then is

$$\frac{d^2\vec{r}}{dt^2} = F(r)\hat{r}. \quad (\text{A.1})$$

Now,

$$\frac{d}{dt} \left( \vec{r} \times \frac{d\vec{r}}{dt} \right) = 0 \quad (\text{A.2})$$

i.e., the motion takes place in a plane and we can simplify our computations by using polar coordinates  $(r, \phi)$  where the center of attraction is at  $r = 0$  and  $\phi$  is the azimuthal angle in the orbital plane. Using the equations for derivatives of the unit vectors

$$\frac{d\hat{r}}{d\phi} = \hat{\phi}; \quad \frac{d\hat{\phi}}{d\phi} = -\hat{r}, \quad (\text{A.3})$$

we get from Eq. (A.1)

$$(\ddot{r} - r\dot{\phi}^2)\hat{r} + (2\dot{r}\dot{\phi} + r\ddot{\phi})\hat{\phi} = F(r)\hat{r}, \quad (\text{A.4})$$

i.e.,

$$\ddot{r} - r\dot{\phi}^2 = F(r) \quad (\text{A.5})$$

$$2\dot{r}\dot{\phi} + r\ddot{\phi} = 0. \quad (\text{A.6})$$

After multiplication with  $r$ , the second equation can be written

$$\frac{d}{dt}(r^2\dot{\phi}) = 0, \quad (\text{A.7})$$

i.e.,

$$r^2\dot{\phi} = \text{constant} \equiv L. \quad (\text{A.8})$$

This can be used to replace  $t$  with  $\phi$  as the independent variable in Eq. (A.5), obtaining

$$\frac{L^2}{r^2} \frac{d}{d\phi} \left( \frac{1}{r^2} \frac{dr}{d\phi} \right) - \frac{L^2}{r^3} = F(r). \quad (\text{A.9})$$

Now, we plug in the explicit form of  $F(r)$  in the case of a point mass

$$F(r) = -\frac{M}{r^2} \quad (\text{A.10})$$

and makes the substitution  $u = 1/r$ , to get

$$\frac{d^2u}{d\phi^2} + u = \frac{M}{L^2}. \quad (\text{A.11})$$

The general solution of this equation is given by

$$u = A \cos(\phi - \phi_0) + \frac{M}{L^2}, \quad (\text{A.12})$$

where  $A$  and  $\phi_0$  are arbitrary constants. Defining the quantity  $p$  as

$$p \equiv \frac{M}{L^2} \quad (\text{A.13})$$

and choosing  $\phi_0 = 0$  [i.e.,  $r_{\min} = r(0)$ ], we get

$$r = \frac{p}{p A \cos \phi + 1}. \quad (\text{A.14})$$

We from this relation we get

$$r_{\min} = \frac{p}{p A + 1}. \quad (\text{A.15})$$

We now introduce Cartesian coordinates in the plane of the orbit according to (see Fig. A.1)

$$x = c - r \cos \phi, \quad y = r \sin \phi. \quad (\text{A.16})$$

From Eqns. (A.14) and (A.16) we get two expressions for  $r^2$ . Equating these we obtain

$$p^2 [1 - A(c - x)]^2 = (c - x)^2 + y^2. \quad (\text{A.17})$$

The constant  $c$  is chosen so that terms linear in  $x$  cancel

$$c = \frac{p^2 A}{p^2 A^2 - 1}, \quad (\text{A.18})$$

and since  $a = c - r_{\min}$ , we can write

$$a = \frac{p}{p^2 A^2 - 1}. \quad (\text{A.19})$$

In terms of these constants, Eq. (A.14) can be written

$$\frac{x^2}{a^2} - \frac{y^2}{c^2 - a^2} = 1, \quad (\text{A.20})$$

or, introducing  $b = \sqrt{c^2 - a^2}$

$$\frac{x^2}{a^2} - \frac{y^2}{b^2} = 1. \quad (\text{A.21})$$

This is the equation for an hyperbola with eccentricity  $\epsilon = c/a = p A$ . Note that  $\epsilon^2 = 1 + \left(\frac{L v}{M}\right)^2$  where  $L = v b$ . We can now calculate the deflection angle  $\alpha$  (see Fig. A.1)

$$\alpha = 2 \arctan \left( \frac{a}{b} \right) \sim \frac{2a}{b}, \quad (\text{A.22})$$

when  $\alpha$  is small. Since  $b = \sqrt{c^2 - a^2}$  we get

$$b = a \sqrt{\epsilon^2 - 1} = a \frac{L v}{M}, \quad (\text{A.23})$$

and for small deflection angles we have

$$\alpha \sim \frac{2M}{b v^2}. \quad (\text{A.24})$$

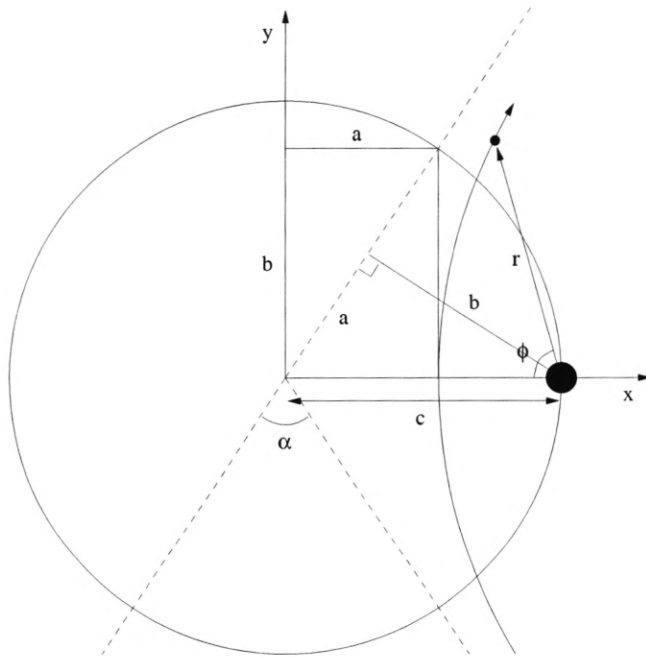


Figure A.1: Geometry of Newtonian deflection

There is in fact an easier way to derive the deflection angle from Eq. (A.14). Note that the maximum angle  $\phi = \phi_{\max}$  is given by

$$\phi_{\max} = \frac{\pi}{2} + \frac{\alpha}{2}. \quad (\text{A.25})$$

Since  $r(\phi_{\max}) = \infty$ , we get

$$\phi_{\max} = \arccos\left(-\frac{1}{pA}\right) = \arccos\left(-\frac{1}{\epsilon}\right) \sim \frac{\pi}{2} + \frac{1}{\epsilon}, \quad (\text{A.26})$$

when the deflection angle is small. That is,

$$\alpha \sim \frac{2}{\epsilon} \sim \frac{2M}{bv^2}. \quad (\text{A.27})$$

Setting  $v = c = 1$ , we see that the deflection angle as calculated in Newtonian gravity is half the deflection angle as calculated in GR.

## Appendix B

# Derivation of the geodesic deviation

In this Appendix, we derive the geodesic deviation equation as used in SNOC when calculating gravitational lensing effects by tracing a light-beam through a series of spherical cells.

We recall the geodesic deviation equation (3.26)

$$\Delta_k \Delta_k \xi^\alpha = -\Delta^\alpha_\beta \xi^\beta. \quad (\text{B.1})$$

We want to study the effect from inhomogeneities not only on two nearby light-rays but on a beam of light. Specifically, we want to study the area of the beam. In order to do this, we write the geodesic equation in two-dimensional form, i.e., in terms of a  $2 \times 2$  matrix  $\mathcal{A}^\alpha_\beta$ , such that

$$\Delta_k \Delta_k \mathcal{A}^\alpha_\beta = -\Delta^\alpha_\gamma \mathcal{A}^\gamma_\beta. \quad (\text{B.2})$$

The area of the beam is given by  $\det \mathcal{A}$ , and the corresponding luminosity will be proportional to the inverse of the area, see Sec. 3 in **Paper I**. In the case of homogeneous cells corresponding to a perfect FL cosmology, we denote the area  $A_{\text{FL}}$ , which will of course depend on the redshift, but also on the cosmological parameters of the background model. The area of a light beam propagating through empty cells will be denoted  $A_{\text{empty}}$ .  $A_{\text{FL}}$  and  $A_{\text{empty}}$  correspond to the filled- and empty-beam distances, respectively.

The deviation equation (B.2) can now be written as a set of difference equations

$$(\mathcal{A}^\alpha_\beta)_1 = (\mathcal{A}^\alpha_\beta)_0 + \Delta\lambda(d\mathcal{A}^\alpha_\beta/d\lambda)_0, \quad (\text{B.3})$$

$$(d\mathcal{A}^\alpha_\beta/d\lambda)_1 = (d\mathcal{A}^\alpha_\beta/d\lambda)_0 - \omega J^\alpha_\gamma (\mathcal{A}^\gamma_\beta)_0, \quad (B.4)$$

where  $\lambda$  is an affine parameter along the light-beam given by  $\omega d\lambda = dt$ , and

$$J^\alpha_\beta = \frac{1}{\omega} \int_c d\lambda \Delta^\alpha_\beta, \quad (B.5)$$

where the integration is along a straight line through the cell.  $\Delta_{\alpha\beta}$  is calculated from the post-Minkowskian line element (5.2). Transforming to co-moving coordinates on isotropic form and including the effects of non-vanishing pressure components, Eq. (5.2) can be written

$$\begin{aligned} ds^2 = & - \left[ 1 + 2\Phi + 4\pi R^2 \sum_i p_i \right] dT^2 \\ & + [1 - 2\Phi] (dX^2 + dY^2 + dZ^2), \end{aligned} \quad (B.6)$$

where  $R^2 \approx X^2 + Y^2 + Z^2$ , and the effective potential

$$\Phi = \phi + \frac{2\pi R^2}{3} \sum_i \rho_i \quad (B.7)$$

satisfies the Poisson equation [cf. Eq. (3.28)]

$$\nabla^2 \Phi = 4\pi \sum_i \rho_i. \quad (B.8)$$

The resulting  $\Delta_{\alpha\beta}$  is given by

$$\Delta_{\alpha\beta} = \omega^2 \left\{ 2\partial_\alpha \partial_\beta \Phi + \left[ Z^a \partial_a (Z^b \partial_b \Phi) + 4\pi \sum_i p_i \right] \eta_{\alpha\beta} \right\}, \quad (B.9)$$

where  $\eta_{ab}$  is the Minkowski metric associated with the coordinates  $(T, X, Y, Z)$ .

### Example: point-mass

Here we show how the  $J^\alpha_\beta$  are calculated for the case of point-mass lenses. Following a light-ray through a cell as depicted in Fig. B.1, we choose our coordinate system such that

$$\begin{aligned} X &= \xi \\ Y &= 0 \\ Z &= \sqrt{r^2 - \xi^2}. \end{aligned} \quad (B.10)$$

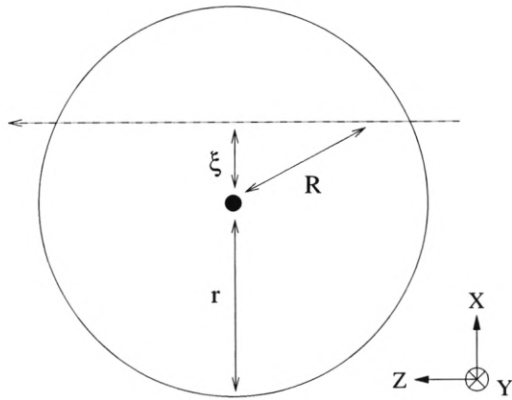


Figure B.1: Cell with point-mass.

We want to compute [cf. Eq. (B.5)]

$$\begin{aligned}
 J^X_X &= \int_{-Z}^Z dZ (2\partial_X^2 \Phi + \partial_Z^2) \\
 J^Y_Y &= \int_{-Z}^Z dZ (2\partial_Y^2 \Phi + \partial_Z^2) \\
 J^X_Y &= \int_{-Z}^Z dZ (2\partial_X \partial_Y \Phi).
 \end{aligned} \tag{B.11}$$

The gravitational potential is given by

$$\Phi = -\frac{M}{R} = -\frac{M}{\sqrt{X^2 + Y^2 + Z^2}}, \tag{B.12}$$

and thus

$$\begin{aligned}
 \partial_X^2 \Phi &= \frac{M}{r^3} \left(1 - 3\frac{\xi^2}{r^2}\right) \\
 \partial_Y^2 \Phi &= \frac{M}{r^3} \left(1 - 3\frac{\xi^2}{r^2}\right) \\
 \partial_Z^2 \Phi &= \frac{M}{r^3} \left(3\frac{\xi^2}{r^2} - 2\right) \\
 \partial_X \partial_Y \Phi &= -3M \frac{XY}{r^5}.
 \end{aligned} \tag{B.13}$$

Performing the integrations in Eq. (B.11), we finally obtain,

$$\begin{aligned} J^X_X &= -2\frac{M}{\xi^2}\sqrt{1-\frac{\xi^2}{r^2}}\left(2+\frac{\xi^2}{r^2}\right) \\ J^Y_Y &= 2\frac{M}{\xi^2}\sqrt{1-\frac{\xi^2}{r^2}}\left(2+\frac{\xi^2}{r^2}\right) \\ J^X_Y &= 0. \end{aligned} \tag{B.14}$$

# Bibliography

- [1] Aguirre, A., ApJ, **512**, L19 (1999).
- [2] Aguirre, A., ApJ, **525**, 583 (1999).
- [3] Aguirre, A., & Haiman, Z., ApJ, **532**, 28 (2000).
- [4] Bahcall, N.A. & Fan, X., ApJ, **504**, 1 (1998).
- [5] Bergström L., & Goobar A., *Cosmology and Particle Astrophysics* (Wiley/Praxis, Chichester, 1999).
- [6] Buchert, T., GRG, **33**, 1381 (2001).
- [7] Burles, S., et al., PRL, **82**, 4176 (1999).
- [8] Cardelli, J.A., Clayton, G.C., & Mathis, J.S., ApJ, **345**, 245 (1989).
- [9] Deffayet, C., Harari, D., Uzan, J.P., & Zaldarriaga, M., arXiv:hep-ph/0112118 (2001).
- [10] Draine, B., & Lee, H., ApJ, **285**, 89 (1984).
- [11] Dyer, C.C., & Roeder, R.C., ApJ, **180**, L31 (1973).
- [12] Einstein, A., Annalen der Physik, **35**, 898 (1911).
- [13] Goliath, M., Amanullah, R., Astier, P., Goobar, A., & Pain, R., A&A, **380**, 6 (2001).
- [14] Goobar, A., & Perlmutter, S., ApJ, **450**, 14 (1995).
- [15] Goobar, A., Mörtsell, E., Amanullah, R., & Nugent, P., in preparation.

- [16] Grasso, D., & Rubinstein, H.R., Phys. Rep., **348**, 163 (2001) [arXiv:astro-ph/0009061].
- [17] Hagmann, C., et al., PRL, **80** 2043 (1998).
- [18] Hatano, K., et al., ApJ, **502**, 177 (1998).
- [19] Holz, D.E. & Wald, R.M., PRD, **58** 063501 (1998).
- [20] Komatsu, E. & Seljak, U., MNRAS, **327**, 1353 (2001).
- [21] Mathis, J.S., Rumpl, W., & Nordsieck, K.H., ApJ, **217**, 425 (1977).
- [22] Milgrom, M., arXiv:astro-ph/0112069 (2001).
- [23] Netterfield, C.B., et al., arXiv:astro-ph/0104460 (2001).
- [24] Ogawa, I., Matsuki, S., & Yamamoto, K., PRD, **53**, R1740 (1996).
- [25] Peacock, J.A., et al., Nature, **410**, 169 (2001).
- [26] Perlmutter, S., et al., ApJ, **517**, 565 (1999).
- [27] Perlmutter, S., et al., the SuperNova Acceleration Probe, <http://snap.lbl.gov>
- [28] Pryke, C., et al., arXiv:astro-ph/0104490 (2001).
- [29] Raffelt G., *Stars as Laboratories for Fundamental Physics* (The University of Chicago Press, Chicago, 1996).
- [30] Riess, A.G., et al., AJ, **116**, 1009 (1998).
- [31] Sakurai, J.J., *Modern Quantum Mechanics*, (Addison-Wesley, Reading, 1995).
- [32] Science Magazine, **282**, 5397 (1998).
- [33] Seljak, U., arXiv:astro-ph/0201450 (2002).
- [34] Seljak, U., & Holz, D., A&A, **351**, L10 (1999).
- [35] Schneider, P., Ehlers, J., & Falco, E.E., *Gravitational Lenses* (Springer-Verlag, New York, 1992).

- [36] Schutz, B.F., *A first course in general relativity*, (Cambridge University Press, Cambridge, 1990).
- [37] Stompor, R., et al., arXiv:astro-ph/0105062 (2001).
- [38] van Bibber, K., et al., PRL, **59**, 759 (1987).
- [39] Wang, X., Tegmark, M. & Zaldarriaga, M., arXiv:astro-ph/0105091 (2001).



# Summary of papers

- I.** The Holz & Wald method for calculating gravitational lensing effects is generalised to matter distributions more accurately reflecting real galaxy properties.
- II.** It is shown that a sample of 100 Type Ia supernovae at  $z \simeq 1$  can be used to discern between the extreme cases of all dark matter in compact objects and smooth dark matter halos.
- III.** The method used in **Paper II** is refined to show how data from one year's operation of the proposed SNAP satellite can be used to determine the fraction of compact objects to  $\lesssim 5\%$  accuracy.
- IV.** Gravitational lensing effects on the observed luminosity of SN1997ff, a Type Ia supernovae at  $z \simeq 1.7$ , are investigated with the result that large magnifications cannot be ruled out with the current knowledge of the foreground galaxies.
- V.** The best-fit value of the homogeneity parameter  $\alpha$  in the Dyer-Roeder distance-redshift relation is determined for a variety of redshifts, inhomogeneity models and cosmological parameter values.
- VI.** The effect of dust on supernova observations is studied. It is shown how 1% relative spectrophotometric accuracy (or broad-band photometry) in the wavelength interval 0.7–1.5  $\mu\text{m}$  can be used to measure the extinction caused by “grey” dust down to  $\delta m = 0.02$  magnitudes.

- VII.** The photon-axion conversion probability is calculated using a density matrix formalism and its effect on Type Ia supernova observations is investigated.
- VIII.** SNOC, the SuperNova Observation Calculator, is presented. This Monte-Carlo package for simulation of supernova observations includes, e.g., effects from gravitational lensing, dust extinction and photon-axion oscillations.
- IX.** Gravitational lensing will cause a bias in the Hubble diagram. In this paper we show how this can be corrected for.



